



# **UNIVERSIDAD DE INVESTIGACIÓN DE TECNOLOGÍA EXPERIMENTAL YACHAY**

**Escuela de Ciencias Biológicas e Ingeniería**

**TÍTULO: Molecular Modeling of the Interaction of Ilmofosine as  
a Therapeutic Agent against Trypanosoma cruzi amastigotes in  
the treatment of Chagas Disease.**

Trabajo de integración curricular presentado como requisito para la  
obtención del título de Ingeniero Biomédico

**Autor:**

Granizo Doumet Gustavo Adib

**Tutora:**

PhD - Lira Vergara Renée Constanza

Urququí, diciembre 2024

# AUTORÍA

Yo, **GRANIZO DOUMET GUSTAVO ADIB**, con cédula de identidad 1313349902, declaro que las ideas, juicios, valoraciones, interpretaciones, consultas bibliográficas, definiciones y conceptualizaciones expuestas en el presente trabajo; así cómo, los procedimientos y herramientas utilizadas en la investigación, son de absoluta responsabilidad de el/la autora (a) del trabajo de integración curricular. Así mismo, me acojo a los reglamentos internos de la Universidad de Investigación de Tecnología Experimental Yachay.

Urcuquí, agosto 2024.

---

Gustavo Adib Granizo Doumet  
CI: 1313349902

# AUTORIZACIÓN DE PUBLICACIÓN

Yo, **GRANIZO DOUMET GUSTAVO ADIB**, con cédula de identidad 1313349902, cedo a la Universidad de Investigación de Tecnología Experimental Yachay, los derechos de publicación de la presente obra, sin que deba haber un reconocimiento económico por este concepto. Declaro además que el texto del presente trabajo de titulación no podrá ser cedido a ninguna empresa editorial para su publicación u otros fines, sin contar previamente con la autorización escrita de la Universidad.

Asimismo, autorizo a la Universidad que realice la digitalización y publicación de este trabajo de integración curricular en el repositorio virtual, de conformidad a lo dispuesto en el Art. 144 de la Ley Orgánica de Educación Superior

Urququí, agosto 2024.

---

Gustavo Adib Granizo Doumet  
CI: 1313349902

# Dedicatoria

A mi familia por siempre apoyarme y brindarme su cariño.

Gustavo Adib Granizo Doumet

# Agradecimiento

Agradezco profundamente a mis docentes y tutores por formarme durante este largo camino e impulsarme a cumplir mis metas.

Gustavo Adib Granizo Doumet

# Resumen

Este estudio investiga la eficacia de la ilmofosina y el ketoconazol, de manera individual y en combinación, contra los amastigotes de *Trypanosoma cruzi*, el agente causante de la enfermedad de Chagas. La investigación abarca enfoques tanto experimentales como computacionales. Se realizaron experimentos *in vitro* utilizando cultivos de células Vero infectadas con tripomastigotes sanguíneos de *T. cruzi*, que posteriormente se desarrollaron en amastigotes. Se probaron diversas concentraciones de ilmofosina y ketoconazol por separado para determinar sus efectos inhibitorios sobre la replicación del parásito, y los resultados demostraron una reducción en el número de amastigotes dependiente de la concentración de los fármacos, observándose una erradicación completa a 1  $\mu\text{M}$  de ilmofosina y 4 nM de ketoconazol. Paralelamente, el tratamiento combinado mostró un efecto sinérgico, inhibiendo completamente con una concentración menor la replicación del parásito en cultivos de células Vero usando 0.2  $\mu\text{M}$  de ilmofosina y 2 nM de ketoconazol.

Además del trabajo experimental, se emplearon simulaciones de modelado molecular y acoplamiento (docking) para elucidar las interacciones entre estos fármacos y las vías metabólicas esenciales para la replicación de *T. cruzi*. La ilmofosina demostró actividad inhibitoria sobre la fosfatidiletanolamina N-metiltransferasa (PEMT) de la vía de transmetilación de Bremer-Greenberg, mientras que el ketoconazol mostró un efecto inhibitorio sobre la esteroil 14 $\alpha$ -desmetilasa (CYP51) y la esteroil 24-C-metiltransferasa de la vía de biosíntesis de ergosterol. Los estudios de acoplamiento revelaron que la combinación de ilmofosina y ketoconazol ejerció un efecto inhibitorio y sinérgico sobre estas enzimas. La integración de los datos experimentales con el modelado computacional ofrece una comprensión integral del potencial terapéutico de la ilmofosina y el ketoconazol en combinación contra el *T. cruzi* y contribuye al desarrollo de estrategias de tratamiento más efectivas para la enfermedad de Chagas.

**Palabras clave:** Ilmofosina, ketoconazol, amastigotes de *Trypanosoma cruzi*, modelado molecular, simulaciones de acoplamiento.

# Abstract

This study investigates the efficacy of ilmofosine and ketoconazole, both individually and in combination, against *Trypanosoma cruzi* amastigotes, the causative agent of Chagas disease. The research encompasses both experimental and computational approaches. *In vitro* experiments were conducted using Vero cell cultures infected with *T. cruzi* blood trypomastigotes, which later developed into amastigotes. Various concentrations of ilmofosine and ketoconazole were tested separately to determine their inhibitory effects on parasite replication and the results demonstrated a drug concentration-dependent reduction in amastigote numbers, with complete eradication observed at 1  $\mu\text{M}$  of ilmofosine and 4 nM of ketoconazole. Furthermore, the combined treatment exhibited a synergistic effect, totally inhibiting at a lower concentration the parasite replication in Vero cell cultures using 0.2  $\mu\text{M}$  of ilmofosine and 2 nM of ketoconazole.

In addition to the experimental work, molecular modeling and docking simulations were employed to elucidate the interactions between these drugs and the metabolic pathways essential for the replication of *T. cruzi*. Ilmofosine demonstrated inhibitory activity on phosphatidylethanolamine N-methyltransferase (PEMT) of the Bremer-Greenberg transmethylation pathway, while ketoconazole showed an inhibitory effect on sterol 14 $\alpha$ -demethylase (CYP51) and sterol 24-C-methyltransferase of the ergosterol biosynthesis pathway. The docking studies revealed that the combination of ilmofosine and ketoconazole exerted an inhibitory and synergistic effect on these enzymes. The integration of experimental data with computational modeling offers a comprehensive understanding of the therapeutic potential of ketoconazole and ilmofosine in combination against *T. cruzi* and contributes to the development of more effective treatment strategies for Chagas disease.

**Key words:** Ilmofosine, ketoconazole, *Trypanosoma cruzi* amastigotes, molecular modeling, docking simulations.

# Contents

<b>Resumen</b>	<b>vi</b>
<b>Abstract</b>	<b>vii</b>
<b>Contents</b>	<b>1</b>
<b>List of Tables</b>	<b>4</b>
<b>List of Figures</b>	<b>6</b>
<b>List of Equations</b>	<b>8</b>
<b>1. Introduction</b>	<b>9</b>
1.1 Background .....	9
1.2 Problem Statement .....	9
1.3 Objectives .....	10
1.3.1 General Objectives .....	10
1.3.2 Specific Objectives .....	10
<b>2. Theoretical Framework</b>	<b>11</b>
2.1 <i>Trypanosoma cruzi</i> Life Cycle .....	11
2.1.1 Infection and Entry into the Mammalian Host .....	11
2.1.2 Intracellular Stage: Amastigotes .....	11
2.1.3 Transformation to Trypomastigotes .....	12
2.1.4 Insect Vector Stage: Epimastigotes .....	12
2.2 Clinical Forms .....	13
2.2.1 Acute Phase .....	13
2.2.2 Chronic Phase .....	13
2.3 Actual Treatment .....	14
2.4 Repositioning of therapeutic drugs and new treatments .....	14
2.4.1 Ilmofosine .....	15
2.4.2 Ketoconazole .....	15
2.5 Therapeutic targets of <i>T. cruzi</i> .....	16



2.5.1 Ergosterol Biosynthesis .....	16
2.5.2 Phosphatidylcholine biosynthesis via the Bremer-Greenberg transmethylation pathway .....	18
2.6 Combination Therapy and Pharmacological Synergism .....	19
2.6.1 Two-way ANOVA .....	19
2.6.2 Bliss Independence Model .....	20
2.6.3 Fractional inhibitory concentration index .....	20
2.6.4 Isobologram analysis .....	20
2.7 Molecular Modeling .....	21
2.7.1 Docking Simulation .....	21
<b>3. Methodology</b> .....	<b>22</b>
3.1 Parasites .....	22
3.2 Drugs .....	22
3.3 <i>In Vitro</i> Studies .....	22
3.4 Staining Solutions .....	23
3.4.1 Fixation and Staining of Slides .....	23
3.5 Synergism Calculations .....	23
3.5.1 Two-way ANOVA .....	23
3.5.2 Bliss Independence Model .....	24
3.5.3 Fractional Inhibitory Concentration Index .....	24
3.6 Molecular Modeling .....	24
3.6.1 Ligand Preparation .....	24
3.6.2 Protein Preparation .....	24
3.6.3 Grid .....	25
3.6.4 Docking Simulation .....	25
3.6.5 Analysis .....	25
<b>4. Results and Discussion</b> .....	<b>26</b>
4.1 Experimental Evidence of Synergy .....	26

4.2 Two-way ANOVA .....	30
4.3 Bliss Independence Model .....	30
4.4 Fractional Inhibitory Concentration Index .....	31
4.5 Comparative Docking Studies of Ilmofosine and Ketoconazole .....	32
4.6 Docking Studies of Both Drugs at the Same Time: Searching for Sinergy ..	38
<b>5. Conclusions</b>	<b>48</b>
<b>6. References</b>	<b>50</b>

# List of Tables

	<b>PAG</b>
1. Two-way ANOVA analysis of drug type, concentration, and their interaction effects on <i>T. cruzi</i> amastigote replication .....	30
2. Interaction Analysis of Ilmofosine and Phosphatidylethanolamine N-methyltransferase from <i>Homo sapiens</i> .....	32
3. Interaction Analysis of Ketoconazole and Phosphatidylethanolamine N-methyltransferase from <i>Homo sapiens</i> .....	33
4. Interaction Analysis of Ilmofosine and Sterol 14 $\alpha$ -demethylase from <i>T. cruzi</i> .....	34
5. Interaction Analysis of Ketoconazole and Sterol 14 $\alpha$ -demethylase from <i>T. cruzi</i> ..	34
6. Interaction Analysis of Ilmofosine and Sterol 24-C-methyltransferase from <i>T. cruzi</i> .....	35
7. Interaction Analysis of Ketoconazole and Sterol 24-C-methyltransferase from <i>T. cruzi</i> .....	36
8. Interaction Analysis of Ilmofosine and Phosphatidylethanolamine N-methyltransferase from <i>Homo sapiens</i> with Ketoconazole bound in its most likely position .....	38
9. Interaction Analysis of Ilmofosine and Phosphatidylethanolamine N-methyltransferase from <i>Homo sapiens</i> with Ketoconazole bound in Asn64 .....	39
10. Interaction Analysis of Ketoconazole and Phosphatidylethanolamine N-methyltransferase from <i>Homo sapiens</i> with Ilmofosine bound in its most likely position .....	39
11. Interaction Analysis of Ketoconazole and Phosphatidylethanolamine N-methyltransferase from <i>Homo sapiens</i> with Ilmofosine bound in Asn64 .....	40
12. Interaction Analysis of Ilmofosine and Sterol 14 $\alpha$ -demethylase from <i>T. cruzi</i> with Ketoconazole bound in Tyr103 .....	41
13. Interaction Analysis of Ilmofosine and Sterol 14 $\alpha$ -demethylase from <i>T. cruzi</i> with Ketoconazole bound in Leu357 .....	42
14. Interaction Analysis of Ketoconazole and Sterol 14 $\alpha$ -demethylase from <i>T. cruzi</i> with Ilmofosine bound in Lys426 .....	42
15. Interaction Analysis of Ketoconazole and Sterol 14 $\alpha$ -demethylase from <i>T. cruzi</i> with Ilmofosine bound in Tyr116 .....	43
16. Interaction Analysis of Ilmofosine and Sterol 24-C-methyltransferase from <i>T. cruzi</i> with Ketoconazole bound in Phe95 .....	44

17.	Interaction Analysis of Ilmofosine and Sterol 24-C-methyltransferase from <i>T. cruzi</i> with Ketoconazole bound in Leu97 .....	45
18.	Interaction Analysis of Ketoconazole and Sterol 24-C-methyltransferase from <i>T. cruzi</i> with Ilmofosine bound in Phe95 .....	45
19.	Interaction Analysis of Ketoconazole and Sterol 24-C-methyltransferase from <i>T. cruzi</i> with Ilmofosine bound in Leu97 .....	46

# List of Figures

	<b>PAG</b>
1. <i>Trypanosoma cruzi</i> Life Cycle .....	12
2. Chemical Structure and Chemical Formula of Ilmofosine .....	15
3. Chemical Structure and Chemical Formula of Ketoconazole .....	16
4. Ergosterol Biosynthesis Pathway .....	17
5. Phosphatidylcholine biosynthesis via the Bremer-Greenberg transmethylation pathway .....	18
6. Impact of different concentrations of Ilmofosine on the replication of <i>T. cruzi</i> amastigotes in Vero cell cultures .....	26
7. Impact of different concentrations of Ketoconazole on the replication of <i>T. cruzi</i> amastigotes in Vero cell cultures .....	27
8. Synergistic effect of Ilmofosine and Ketoconazole on the replication of <i>T. cruzi</i> amastigotes in Vero cell cultures .....	28
9. Dose-response curve of Ilmofosine on the replication of <i>T. cruzi</i> amastigotes per cell .....	28
10. Dose-response curve of ketoconazole on the replication of <i>T. cruzi</i> amastigotes per cell .....	29
11. Dose-response curve of Ketoconazole at 2 nM combined with Ilmofosine on the replication of <i>T. cruzi</i> amastigotes per cell .....	29
12. Isobologram curve describing the synergistic effect of Ilmofosine and Ketoconazole on <i>T. cruzi</i> amastigotes replication .....	32
13. Most likely binding position of Ilmofosine and Phosphatidylethanolamine N-methyltransferase from Homo sapiens .....	33
14. Most likely binding position of Ketoconazole and Phosphatidylethanolamine N-methyltransferase from Homo sapiens .....	33
15. Most likely binding position of Ilmofosine and Sterol 14 $\alpha$ -demethylase from <i>T. cruzi</i> .....	34
16. Most likely binding position of Ketoconazole and Sterol 14 $\alpha$ -demethylase from <i>T. cruzi</i> .....	35
17. Most likely binding position of Ilmofosine and Sterol 24-C-methyltransferase from <i>T. cruzi</i> .....	35

18.	Most likely binding position of Ketoconazole and Sterol 24-C-methyltransferase from <i>T. cruzi</i> .....	36
19.	Strongest interaction of Ilmofosine and Phosphatidylethanolamine N-methyltransferase from Homo sapiens with Ketoconazole bound in its most likely position .....	38
20.	Strongest interaction of Ilmofosine and Phosphatidylethanolamine N-methyltransferase from Homo sapiens with Ketoconazole bound to a common Hydrogen Bond site .....	39
21.	Strongest interaction of Ketoconazole and Phosphatidylethanolamine N-methyltransferase from Homo sapiens with Ilmofosine bound in its most likely position .....	40
22.	Strongest interaction of Ketoconazole and Phosphatidylethanolamine N-methyltransferase from Homo sapiens with Ilmofosine bound to a common Hydrogen Bond site .....	40
23.	Strongest interaction of Ilmofosine and Sterol 14 $\alpha$ -demethylase from <i>T. cruzi</i> with Ketoconazole bound in its most likely position .....	41
24.	Strongest interaction of Ilmofosine and Sterol 14 $\alpha$ -demethylase from <i>T. cruzi</i> with Ketoconazole bound in its second most likely position .....	42
25.	Strongest interaction of Ketoconazole and Sterol 14 $\alpha$ -demethylase from <i>T. cruzi</i> with Ilmofosine bound in its most likely position .....	43
26.	Strongest interaction of Ketoconazole and Sterol 14 $\alpha$ -demethylase from <i>T. cruzi</i> with Ilmofosine bound in its second most likely position .....	43
27.	Strongest interaction of Ilmofosine and Sterol 24-C-methyltransferase from <i>T. cruzi</i> with Ketoconazole bound in its most likely position .....	44
28.	Strongest interaction of Ilmofosine and Sterol 24-C-methyltransferase from <i>T. cruzi</i> with Ketoconazole bound to a common Hydrogen Bond site .....	45
29.	Strongest interaction of Ketoconazole and Sterol 24-C-methyltransferase from <i>T. cruzi</i> with Ilmofosine bound in its most likely position .....	46
30.	Strongest interaction of Ketoconazole and Sterol 24-C-methyltransferase from <i>T. cruzi</i> with Ilmofosine bound to a common Hydrogen Bond site .....	46

# List of Equations

	<b>PAG</b>
1. Bliss Independence Model Expected Combination Effect .....	20
2. Fractional Inhibitory Concentration Index based on Loewe's additivity model .....	20

## **1. Introduction**

### **1.1 Background**

Chagas disease (CD), also referred to as American trypanosomiasis, is a long-lasting, widespread disease caused by the protozoan parasite *Trypanosoma cruzi* (1,2). It is classified by the World Health Organization (WHO) as a neglected tropical disease (3), Chagas disease remains a significant public health issue, particularly in Latin America, where it ranks among the leading causes of heart failure (4,5). The parasite infects humans and various species of wild and domestic animals, primarily through bloodsucking reduviid insects of the Triatominae subfamily. Competent vectors such as *Triatoma infestans*, *Rhodnius prolixus*, and *Triatoma dimidiata* are responsible for the transmission of *T. cruzi* through domestic, peridomestic, and wild cycles (1,2).

In addition to insect vectors, *T. cruzi* can also be transmitted through blood transfusions, from mother to child during childbirth, and occasionally through contaminated food or beverages (6). The WHO estimates that *T. cruzi* infects 6 to 8 million people worldwide, leading to approximately 28,000 new cases and between 14,000 and 50,000 deaths each year. This disease significantly burdens global health, putting approximately 70 to 100 million people at risk of infection (3). Despite the prevalence, detection rates in many countries are alarmingly low, often below 10% and sometimes even under 1%. Patients frequently face significant obstacles to obtaining proper diagnosis and adequate healthcare (7).

### **1.2 Problem Statement**

Although more than a century has elapsed since its discovery, CD continues to be a major public health issue in many Latin American countries. In recent years, CD has also emerged as a concern in non-endemic regions, including Canada, the USA, Europe, Australia, and Japan, largely due to the migration of individuals from endemic areas. In these non-endemic regions, transmission occurs mainly through blood transfusion, organ transplantation, or vertical transmission from mother to child (4).

Chronic Chagas disease is considered a disabling disease responsible for significant morbidity and mortality among parasitic diseases, leading to a global expenditure of USD\$627.5 million per year in healthcare costs (4,6). The spread of CD cases worldwide and its status as a global public health concern underlines the need for continued research and development of new therapeutic strategies.



## **1.3 Objectives**

### **1.3.1 General Objectives**

To evaluate the efficacy of ketoconazole and ilmofosine, individually and in combination, against *Trypanosoma cruzi* amastigotes and to elucidate their molecular interactions through computational modeling to develop a more effective treatment strategy for Chagas disease.

### **1.3.2 Specific Objectives**

To evaluate the efficacy of ketoconazole and ilmofosine at different concentrations in eradicating *Trypanosoma cruzi* amastigotes, both individually and in combination, and to investigate their synergistic effects. Additionally, to utilize molecular modeling techniques to study the interactions of ketoconazole, ilmofosine, and their combination with *T. cruzi* amastigotes, and correlate these computational results with experimental findings to gain insights into their mechanisms of action and potential therapeutic benefits.

## **2. Theoretical Framework**

### **2.1 *Trypanosoma cruzi* Life Cycle**

*Trypanosoma cruzi*, the causative agent of Chagas disease, follows a complex life cycle (Figure 1) involving two hosts: a mammalian host and an insect vector. The life cycle encompasses four main stages: metacyclic trypomastigotes, amastigotes, bloodstream trypomastigotes, and epimastigotes (8–11).

The intracellular amastigote stage is particularly important, as it is during this phase that the parasite replicates within the mammalian host, which is essential for its survival and proliferation (8). Our research focuses on this stage to determine the effectiveness of ketoconazole and ilmofosine. By testing these drugs on cells infected with amastigotes, we aim to assess their potential to eliminate the intracellular forms of *T. cruzi*. This approach directly measures the impact of these compounds on parasite replication, a critical aspect in the development of effective treatments for Chagas disease.

#### **2.1.1 Infection and Entry into the Mammalian Host**

The life cycle starts when a triatomine insect vector, often called the "kissing bug," feeds on blood and deposits metacyclic trypomastigotes in its feces near the bite wound. These trypomastigotes can enter the host through the bite wound itself or intact mucous membranes like the conjunctiva (11).

#### **2.1.2 Intracellular Stage: Amastigotes**

Once inside the host, the trypomastigotes invade a variety of nucleated cells near the site of inoculation (11). They bind to receptors on both phagocytic and non-phagocytic cells and enter a membrane-bound vacuole called a parasitophorous vacuole (PV). Within the PV, the trypomastigotes differentiate into small, round-shaped amastigotes and escape into the cell cytoplasm, where they undergo morphological transformation, including flagellar involution (2).

The amastigotes then re-enter the cell cycle and multiply by binary fission (11). They proliferate until the host cell is filled with replicative forms. The intracellular amastigotes measure between 2 to 6.5  $\mu\text{m}$  in diameter and are characterized by the absence of an external flagellum and an undulating membrane (10). Their kinetoplast is located near the nucleus, in an anterior position. Amastigotes provoke the rupture of infected cells, releasing the parasites into the extracellular environment (2,5).

### 2.1.3 Transformation to Trypomastigotes

The intracellular amastigotes then elongate, reacquire their long flagella, and differentiate into non-replicative trypomastigotes (10). These trypomastigotes induce the lysis of the host cell membrane, allowing them to be released into the bloodstream and lymphatic system. As bloodstream trypomastigotes (BTs), they can invade adjacent cells or disseminate throughout the host's body. Unlike the African trypanosomes, bloodstream trypomastigotes of *T. cruzi* do not replicate in the bloodstream. The parasites resume replication only when they infect a new host cell or are ingested by another vector (11).

### 2.1.4 Insect Vector Stage: Epimastigotes

When a triatomine vector feeds on the blood of an infected host, it ingests the bloodstream trypomastigotes. Inside the vector's midgut, the trypomastigotes transform into epimastigotes, which are replicative forms. The epimastigotes multiply and differentiate in the midgut, eventually migrating to the vector's hindgut (8). Here, they attach to the waxy gut cuticle by their flagella and differentiate into infective metacyclic trypomastigotes. These are the forms that are released in the vector's feces, completing the cycle (9).

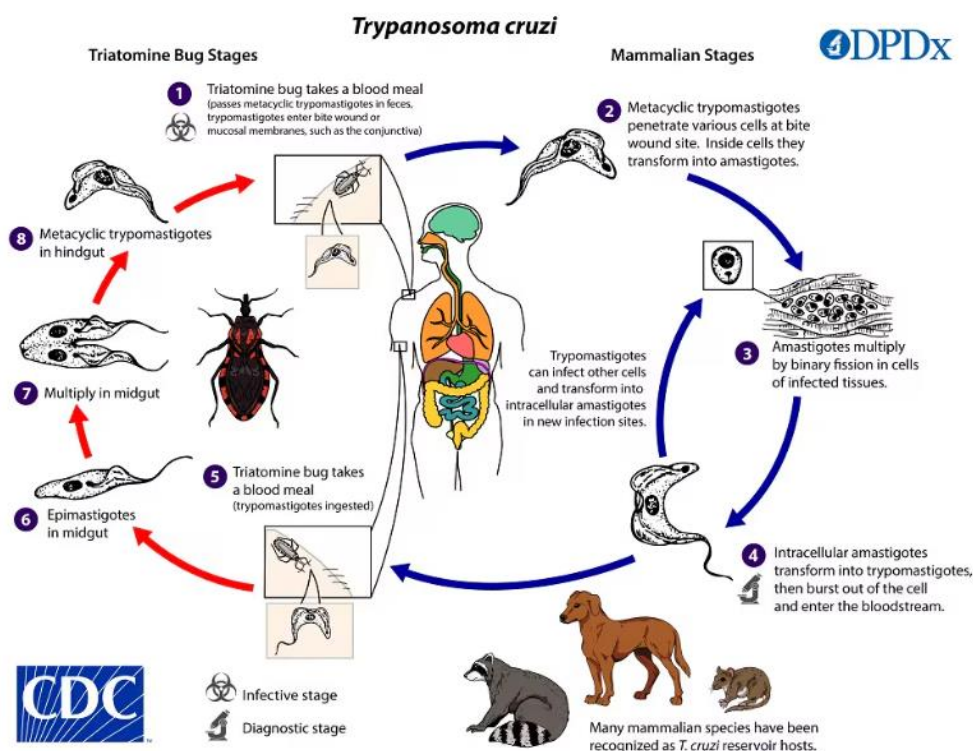


Figure 1: *Trypanosoma cruzi* Life Cycle. Taken from: Centers for Disease Control and Prevention (CDC), Division of Parasitic Diseases and Malaria (DPDM) Training website (DPDX).

## **2.2 Clinical Forms**

*Trypanosoma cruzi* is a protozoan parasite that causes lifelong infections in humans, leading to Chagas disease. The disease typically begins with a brief acute phase, often without symptoms, and progresses to a chronic phase with various clinical manifestations if not treated early (12).

### **2.2.1 Acute Phase**

After the initial infection with *T. cruzi*, the acute phase is characterized by high level of parasite presence in the bloodstream, often without clear symptoms, leading to frequent underdiagnosis during this period (13,14). When symptoms do appear, they can include prolonged fever, headache, muscle pain (myalgia), swollen lymph nodes (lymphadenitis), enlarged liver (hepatomegaly), and enlarged spleen (splenomegaly) (4,7,14). These symptoms typically resolve within 60 days without the use of specific etiological treatments (4,14).

In cases of vector transmission, the infected individual may exhibit clinical signs at the site of parasite entry. For instance, a chagoma can form when the entry occurs through the skin, or Romana's sign can appear if the entry is through the periorbital mucosa (4,14). After 4 to 8 weeks, parasitemia decreases, and in 90% of cases, the clinical symptoms spontaneously disappear, marking the transition to the chronic phase (4).

### **2.2.2 Chronic Phase**

The chronic phase can remain clinically silent for life in 60-70% of infected individuals, known as the asymptomatic or indeterminate form of CD. However, 10-30 years after the initial infection, about 30-40% of asymptomatic patients will develop clinical manifestations. These can include rare neurological symptoms, digestive issues such as megacolon and megaesophagus, and cardiac or cardiodigestive problems (4,14,15).

Cardiac involvement is the most severe manifestation, affecting approximately one-third of infected individuals during their lifetime. Chronic chagasic cardiomyopathy (CCC) is characterized by diffuse myocarditis, fibrosis, and segmental wall motion abnormalities. The late stage of the disease often results in dilated cardiomyopathy with progressive heart failure, and sudden death (4,7,15).

The digestive form of CD results from the denervation of the enteric nervous system, which impairs the motor functions of the digestive tract. This leads to symptoms like dysphagia (difficulty swallowing) and massive constipation due to colon dilation. When both megacolon and megaesophagus occur along with CCC, the condition is termed the cardiodigestive form, which has a particularly poor prognosis (4,14).

### **2.3 Actual Treatment**

Early detection of Chagas disease is crucial because it can be cured if treated promptly after infection. Without timely diagnosis and treatment, the infection can progress to a severe, life-threatening condition requiring lifelong care. This highlights the need for effective therapeutic strategies to combat Chagas disease and prevent its serious consequences (7).

Chagas disease is currently treated with two drugs: benznidazole and nifurtimox. These medications, which have been in use for over 50 years, present several disadvantages. They are only effective during the acute or early phases of infection and often cause significant adverse effects (16–18). These side effects include anorexia, nausea, vomiting, headache, central nervous system depression or manic symptoms, seizures, vertigo, paresthesia, peripheral polyneuropathies, and dermatitis, leading to therapy discontinuation in 10–30% of treated patients. Moreover, different parasite strains have developed resistance to these drugs, complicating treatment further and contributing to treatment failures (17).

Despite the challenges, ongoing research is dedicated to finding new, safe, and effective treatments for Chagas disease. Unfortunately, interest from both governmental bodies and the pharmaceutical industry has been limited. In response, various institutions and research groups have stepped in to lead the charge. They are exploring strategies such as optimizing traditional drug dosages, repurposing existing medications, and developing combination therapies. These efforts are vital for improving treatment options and outcomes for those affected by this neglected tropical disease (17).

### **2.4 Repositioning of Therapeutic Drugs and New Treatments**

Drug repurposing and re-dosing regimens for existing medications, either as monotherapy or in combination therapy, represent the quickest interventions to enhance Chagas disease treatment. These strategies can significantly reduce the costs and time required for developing new medicines because they benefit from prior pharmacokinetic and toxicological studies. The repositioning of existing pharmacotherapeutic agents with known efficacy and safety profiles is regarded as a valuable approach for creating new treatments for a range of diseases, including neglected conditions such as Chagas disease. This approach is advantageous given the cost and time savings compared to developing new medicines from scratch, as the toxicological and pharmacokinetic profiles of these drugs have already been evaluated for their original therapeutic targets (19–21).

Furthermore, the use of two or more pharmaceutical compounds concurrently or sequentially is a promising strategy being explored in Chagas disease treatment studies. Combining different compounds theoretically allows for the reduction of doses and/or treatment duration, thereby minimizing adverse side effects and costs. Synergistic treatments generally enhance the activity of compounds with distinct mechanisms of action, reduce drug toxicity, and lower the risk of developing resistance (19–21).

### 2.4.1 Ilmofosine

Alkyl-lysophospholipids (ALPs), such as ilmofosine (Figure 2), edelfosine, and miltefosine, are synthetic derivatives analogous to lysophospholipids and have been extensively researched for their use in cancer chemotherapy. These compounds have shown effectiveness against *Trypanosoma cruzi* and other trypanosomatids in both *in vitro* and *in vivo* studies (22,23). ALPs act as phospholipid inhibitors by specifically blocking *T. cruzi* phosphatidylcholine (PC) biosynthesis through the Bremer-Greenberg transmethylation pathway, as opposed to the Kennedy CDP-choline pathway used in vertebrate hosts (23).

Ilmofosine also demonstrates significant *in vitro* antiproliferative activity against both promastigotes and intracellular amastigotes of *Leishmania donovani*, which, like *Trypanosoma cruzi*, belongs to the Trypanosomatidae family (24).

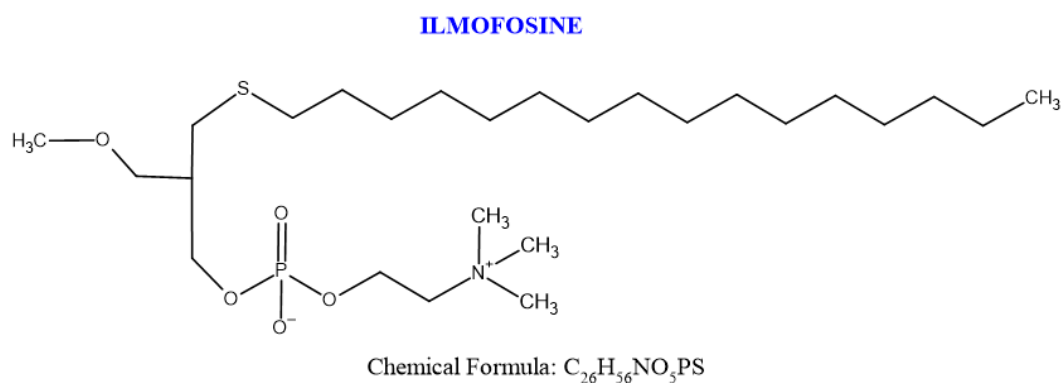


Figure 2: Chemical Structure and Chemical Formula of Ilmofosine. Own authorship.

### 2.4.2 Ketoconazole

Ketoconazole (Figure 3), an imidazole antifungal, has been used in human antifungal treatment for years due to its favorable pharmacokinetic and safety profiles (17). Like many azoles, ketoconazole blocks the biosynthesis of ergosterol, essential for parasite survival, by inhibiting sterol C14-demethylase (17,25–27). Significant efforts have been made to repurpose ketoconazole and other azole antifungals for Chagas disease treatment. It has been evaluated both *in vitro* and *in vivo* against trypanosomatids. These studies revealed that ketoconazole effectively prevents replication inside cells but does not inhibit the extracellular forms of the parasite (27). By inhibiting ergosterol synthesis, ketoconazole demonstrates potent intrinsic activity against *Trypanosoma cruzi*. Although ketoconazole showed *in vitro* efficacy against *T. cruzi*, it failed to cure patients with chronic Chagas disease (17).

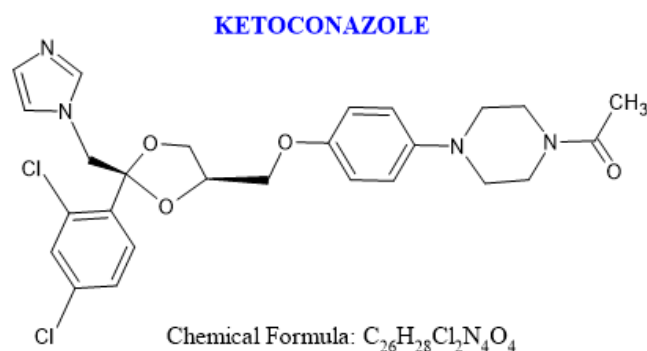


Figure 3: Chemical Structure and Chemical Formula of Ketoconazole. Own authorship.

## 2.5 Therapeutic Targets of *T. cruzi*

For a protein to be considered a therapeutic target, it must meet several criteria. Firstly, there must be genetic and chemical evidence proving that the target is essential for the parasite's growth or survival (17,28). Additionally, the target should have a druggable active site, meaning it can be modulated by both small drug-like compounds and large molecules, such as therapeutic proteins, peptides, monoclonal antibodies, vaccines, among others. These large agents can exert highly specific effects on the target, making them valuable in various therapeutic applications (17,29).

Moreover, proteins that are essential for the parasite stages present in the host should be prioritized. Validation of these targets is necessary by demonstrating that disrupting or deleting the relevant genes causes cell death. This ensures that the target is crucial for the parasite's survival (28). To minimize toxicity, targets should ideally be present in the parasite but have no human homologs, or if human homologs exist, they should be non-essential. Furthermore, the target should have no known isoforms within the same species to reduce the likelihood of resistance development (17).

We subsequently identified two metabolic pathways critical for parasite survival: (a) ergosterol biosynthesis and (b) phosphatidylcholine biosynthesis via the Bremer-Greenberg transmethylation pathway.

### 2.5.1 Ergosterol Biosynthesis

Sterols are essential lipids produced by all eukaryotic cells, playing crucial roles in organizing and functioning of cell membranes. In trypanosomes, the primary sterol component is ergosterol (28). Ergosterol is vital for membrane stabilization, determining membrane permeability and fluidity, and modulating the activity of membrane-bound enzymes and ion channels. This sterol is essential for forming viable membranes and various regulatory processes necessary for parasite growth, development, and division. Unlike mammals, *T. cruzi* cannot accumulate ergosterol from the host, relying entirely on endogenously produced ergosterol (Figure 4). Therefore, blocking ergosterol production is

lethal for the parasite (30). Importantly, the amastigote form of the parasite, which is clinically significant, shows high sensitivity to pharmacological inhibition of this lipid (28).

Sterol 14 $\alpha$ -demethylase (CYP51) is a highly conserved haemoprotein and part of the cytochrome P450 superfamily. This enzyme acts at the initial stages of the sterol biosynthesis pathway, and its inhibition by azoles has been extensively tested and studied (30). A promising yet relatively unexplored strategy involves inhibiting the last enzyme of the ergosterol synthesis pathway, sterol 24-C-methyltransferase (Tc24SMT), using azasterols. Tc24SMT is absent in humans, making it an attractive target. Interestingly, amastigotes are more susceptible than epimastigotes to these compounds (28).

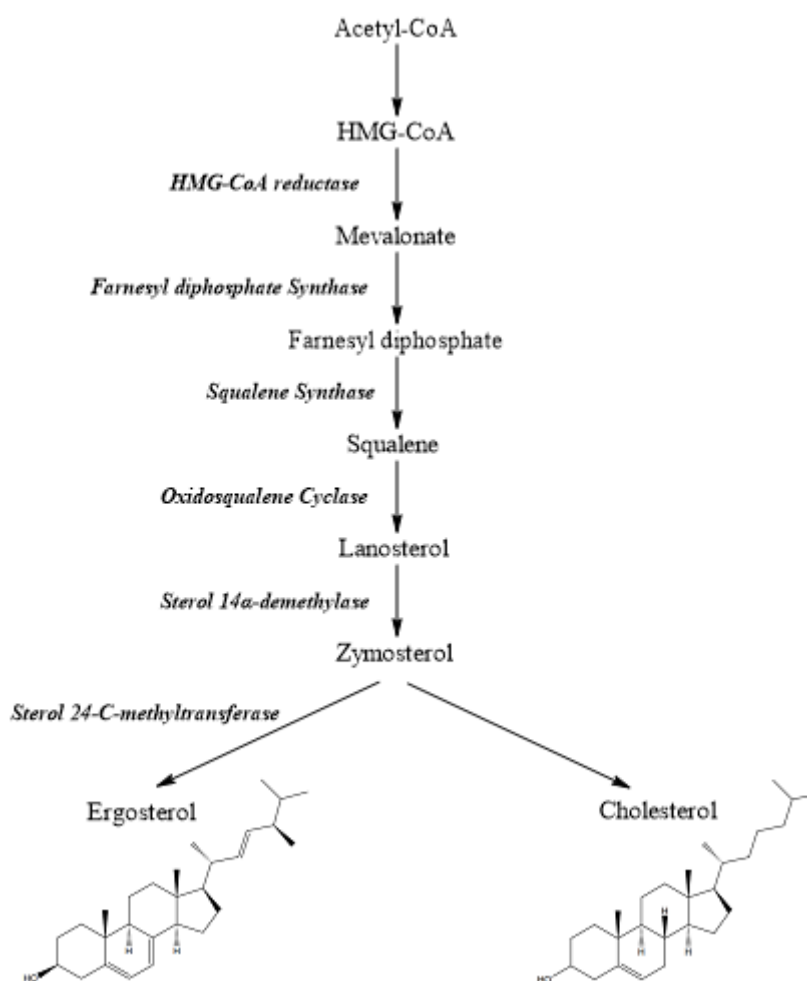


Figure 4: Ergosterol Biosynthesis Pathway. Own authorship.



## 2.5.2 Phosphatidylcholine Biosynthesis via the Bremer-Greenberg Transmethylation Pathway

In certain organisms, including protozoan parasites like *Trypanosoma cruzi*, the Bremer-Greenberg transmethylation pathway (Figure 5) is crucial for producing phosphatidylcholine (PC), a major phospholipid component of cell membranes (23,31). This pathway supports membrane fluidity, integrity, and the function of membrane-bound proteins (31,32).

This pathway involves the methylation of phosphatidylethanolamine (PE) to form PC. This process is mediated by a series of methylation reactions where S-adenosylmethionine (SAM) serves as the methyl donor (32). A key enzyme in this pathway is phosphatidylethanolamine N-methyltransferase (PEMT), which catalyzes the methylation of PE to form monomethyl-PE, dimethyl-PE, and ultimately PC (32).

*Trypanosoma cruzi* relies heavily on the Bremer-Greenberg transmethylation pathway for its survival and proliferation, in contrast to mammalian cells, which primarily use the Kennedy (CDP-choline) pathway for PC synthesis (31–34). This unique reliance makes the pathway an appealing target for therapeutic interventions, as disrupting PC biosynthesis could compromise the parasite's membrane integrity and function (31,32). Inhibiting PEMT, the enzyme responsible for catalyzing the methylation steps in this pathway, may lead to selective toxicity against the parasite while sparing host cells. The importance of this pathway in parasite biology has driven research efforts aimed at finding compounds that can selectively inhibit PEMT, with the goal of developing new treatments for diseases such as Chagas disease (32).

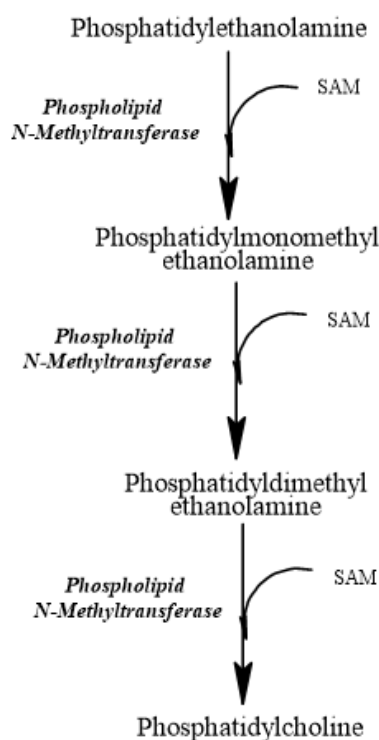


Figure 5: Phosphatidylcholine biosynthesis via the Bremer-Greenberg transmethylation pathway. Own authorship.

## 2.6 Combination Therapy and Pharmacological Synergism

Drug combination is a strategy proposed to overcome the limitations of monotherapy, with several studies demonstrating the superiority of combined therapies (35–40). The primary goal of designing and evaluating drug combinations is to achieve synergistic effects, where the combined effects are significantly greater than the additive effects of the individual drugs (40). Evidence suggests that combinations of drugs are more likely to be synergistic if they are of different classes, have independent mechanisms of action, or act upon different stages of the parasite life cycle (39). Synergistic treatments, which involve compounds with different mechanisms of action, generally improve trypanocidal activity and could increase efficacy to achieve a sterile parasitological cure (20). Additionally, by exploiting the susceptibility of different molecular pathways involved in disease genesis, this approach aims to improve treatment efficiency, reduce cytotoxicity to normal cells, and diminish the development of drug resistance (35–38,40).

To effectively demonstrate the advantages of combining drugs over using them individually, we will use a two-way ANOVA test to assess the statistical significance of the independent and combined effects of the drugs. Additionally, the Bliss independence model will be applied to demonstrate synergism when the drugs act through different mechanisms of action. Finally, the Fractional Inhibitory Concentration Index (FICI) will quantify the level of synergism. This comprehensive approach will highlight the improved efficacy of drug combinations.

### 2.6.1 Two-way ANOVA

Two-way ANOVA is a statistical method used to assess the impact of two independent factors on a dependent variable. It is particularly useful for understanding the individual effects of each factor, known as main effects, as well as how the combination of the two factors influences the dependent variable, referred to as the interaction effect. Additionally, it helps determine whether an interaction exists between the two factors (41,42).

In our study, Two-way ANOVA enables us to evaluate whether the type of drug (ilmofosine, ketoconazole, or their combination) significantly affects the replication of *T. cruzi* amastigotes. It also allows us to investigate whether the concentration of these drugs influences the outcome, and whether the interaction between drug type and concentration results in a significantly different effect than what would be expected from considering each factor individually.

These considerations lead us to define the following null hypotheses:

1. Drug type has no effect on the outcome.
2. Concentration has no effect on the outcome.
3. There is no interaction between drug type and concentration.

It is important to consider that the alternative hypotheses will be the opposite of the null hypotheses.

### 2.6.2 Bliss Independence Model

The Bliss independence model is commonly used for analyzing drug combination data, particularly when screening potential drug combinations. It assumes that two drugs act independently, so their combined effect is expected to be the sum of their individual effects. To evaluate synergy, the observed combined effect is compared to the expected one. If the observed effect exceeds the expected value, this indicates synergy (43).

Mathematically, the expected effect of the combination ( $E_{AB}$ ) can be calculated as:

$$E_{AB} = E_A + E_B - (E_A \times E_B) \quad \text{Eq1}$$

Where,  $E_A$  represents the effect of drug A alone, and  $E_B$  the effect of drug B alone.

### 2.6.3 Fractional Inhibitory Concentration Index

In laboratory environments, the interaction of compounds is typically measured using the fractional inhibitory concentration index (44). This index is calculated by adding the FICs of each drug tested, which are determined by dividing the minimum inhibitory concentration (MIC) of the drug when used in combination by the MIC of the drug when used alone (44–46). MIC refers to the lowest concentration that can visibly inhibit microorganism growth (44). Mathematically, the FICI is expressed as:

$$FICI = FIC_A + FIC_B = \frac{C_A}{MIC_A} + \frac{C_B}{MIC_B} \quad \text{Eq2}$$

In this equation (Eq2), the denominators represent the minimum inhibitory concentrations of drugs A and B, respectively, while the numerators are the concentration of each drug inhibiting parasite growth in combination. Based on Loewe's additivity model, a FICI of 1 denotes an additive effect. A FICI below 1 indicates a synergistic effect, whereas above 1 signifies antagonism (44–46). This implies that a smaller or larger amount of the drug is needed to achieve the same effect as when the drugs are used individually.

### 2.6.4 Isobologram Analysis

Isobologram analysis is a visual method based on Loewe's Additivity model, which facilitates the interpretation of the interaction between two drugs in a combination. This graphical tool plots the doses of drug A and drug B on the x and y axes, respectively (40,47).

In the isobologram, the additive effect is represented by a line with a negative slope, known as the additive isobole. When a data point representing the drug combination falls below this line, it indicates synergy ( $FICI < 1$ ), meaning the drugs enhance each other's effects and require lower doses to achieve the desired outcome. A point on the line indicates additivity ( $FICI = 1$ ), where the combined effect matches the sum of the individual drug effects. Conversely, if the point lies above the line, it suggests antagonism ( $FICI > 1$ ), implying that higher doses are needed to achieve the expected effect due to interference between the drugs. This visual representation on the isobologram offers an intuitive interpretation of drug interactions that corresponds directly to FICI values (40,47).

## 2.7 Molecular Modeling

Computer-aided drug discovery (CADD) is a highly efficient method for reducing the costs associated with new drug development. It identifies target proteins and searches for ligands involved in the metabolism of *Trypanosoma cruzi*. CADD can also predict absorption, distribution, metabolism, excretion, and toxicity (ADMET) profiles, potentially reducing drug discovery costs by 50%. Many researchers have embraced this promising strategy, focusing on inhibiting proteins or enzymes previously validated as potential *T. cruzi* targets (48,49).

Despite the complexities of computational target selection, identifying proteins that meet specific criteria can significantly expedite the drug development process and streamline target-based screenings. The use of freely available bioinformatics tools, such as molecular docking, is essential for rapidly analyzing interactions between therapeutic targets and ligands. Docking simulations are particularly valuable for predicting drug-target binding and providing insights into a drug's mechanism of action. This crucial step helps ensure that only the most promising candidates proceed to in vivo pre-clinical evaluation, thereby improving the overall efficiency of the drug development process (48,50).

### 2.7.1 Docking Simulation

In modern drug discovery efforts, protein-ligand docking simulations play a crucial role by predicting the binding affinity of a ligand to a protein and the strength of this bond (48,51,52). This computational technique has proven effective in identifying potential drugs against *T. cruzi*, offering a cost-effective alternative to traditional experimental screening methods (48,51). Through virtual screening, compounds undergo computational ranking based on docking simulations, prioritizing those likely to bind to the target protein for subsequent biological testing (48).

The virtual screening process typically involves several key steps: first, preparing the protein structure and determining suitable docking sites; second, preparing the compound structures for simulation; and finally, executing the docking simulations themselves (48). These steps are integral to our project, where molecular docking studies are employed to elucidate the binding strength and ligand-interaction profiles through the binding and intermolecular energy of complexes formed between ligands and specific experimental protein 3D structures.

According to Sakyi et al. (53) compounds with binding energies of  $\leq -7.0$  kcal/mol have demonstrated significant inhibitory activities against parasite activity. Lower values indicate stronger binding, with the strength of the binding increasing as the energy value decreases. Additionally, the AutoDockTools user guide classifies intermolecular energy values less than -10 kcal/mol as indicative of strong binding interactions (54,55).

### **3. Methodology**

The research protocol begins with evaluating ketoconazole's effectiveness at various concentrations, followed by a similar evaluation of ilmofosine. Subsequently, the synergistic potential of combining ketoconazole and ilmofosine is investigated to enhance amastigote eradication.

In addition to experimental assessments, molecular modeling is employed to elucidate the interactions between these compounds and different enzymes essential for parasite survival such as: Phosphatidylethanolamine N-methyltransferase, sterol 14 $\alpha$ -demethylase and 24-C-methyltransferase. This modeling process unfolds across three stages: an initial exploration involving ketoconazole, followed by detailed analysis with ilmofosine, and finally, an investigation into their combined effects. The integration of experimental and computational approaches aims to provide molecular insights into the mechanisms of action, thereby contributing to the development of more effective therapeutic strategies against Chagas disease.

The following procedure was realized before obtaining the results:

#### **3.1 Parasites**

The EP (DTU *T. cruzi* I stock, Dm28c strain) and Y (DTU *T. cruzi* II stock, Y strain) strains of *T. cruzi* were utilized in this research. Live *T. cruzi* handling was conducted in accordance with established biosecurity protocols.

#### **3.2 Drugs**

Ilmofosine, supplied by Dr. Simon Croft from the London School of Hygiene and Tropical Medicine (UK), and ketoconazole, sourced from Jansem Pharmaceutica in Caracas, Venezuela, were used in the study. Both drugs were prepared in solutions using dimethylsulphoxide (DMSO), ensuring the final concentration of DMSO in the culture medium remained below 1% (v/v). At this concentration, DMSO did not have any independent effect on the replication of either the parasites or the Vero cells.

#### **3.3 In Vitro Studies**

Amastigote cultures proliferating in Vero cells were sustained in minimal essential medium (MEM, Gibco BRL Cat. No. 41500-067) supplemented with 10% fetal bovine serum (FBS) that was heat-inactivated by incubation at 56°C for 30 minutes to deactivate complement proteins and other interfering factors. After heat inactivation, the serum was rapidly cooled by transferring it into an ice bath for 30 minutes to complete the process. The cultures were incubated in a 95% air, 5% CO<sub>2</sub> atmosphere at 37°C. Cells were exposed to trypomastigotes from cell cultures at a ratio of 10 trypomastigotes per cell for 2 hours. Following this, three washes with phosphate-buffered saline (PBS) were performed to eliminate non-adherent parasites. Fresh medium, either containing or lacking drugs, was subsequently added, and the cells were incubated for 96 hours, with a medium change occurring at the 48-hour mark. The quantification of infected cells and the parasite load per cell was conducted using light

microscopy and statistical analysis. The stained samples were examined at a magnification of 400X (objective lens 40X).

### **3.4 Staining Solutions**

The staining buffer is prepared by mixing 28 ml of sodium phosphate stock solution with 12 ml of potassium phosphate stock solution (11.80 g/l of Na<sub>2</sub>HPO<sub>4</sub>·12H<sub>2</sub>O and 9.07 g/l of KH<sub>2</sub>PO<sub>4</sub>), and all solutions are stored at 4°C. The Giemsa solution, which must be prepared fresh at the time of use, is made by combining 32 ml of staining buffer with 8 ml of Giemsa (Riedel de Haen Ag Seelse-Hannover, Azur-eosin methylene blue Cat. 32884), and the mixture is then filtered through Whatman #1 filter paper. The May-Grunwald solution is prepared by dissolving 0.2 g of May-Grunwald in 100 ml of analytical methanol and storing it in a dry oven at 37°C until needed. Before use, it is heated for approximately 30 minutes in a 50°C water bath and shaken, and then is stored in an amber bottle with a rubber stopper, with a needle through the stopper to prevent it from popping out.

#### **3.4.1 Fixation and Staining of Slides**

The slides were fixed with PBS containing 2.5% glutaraldehyde, washed with PBS, and immersed in absolute methanol for 3 minutes. Staining was carried out with May-Grunwald solution for 5 minutes, rinsed with distilled water, followed by Giemsa staining for 10 minutes, and another wash with distilled water. The slides were then dried, mounted on slide holders with a drop of Canada balsam, ensuring no bubbles were present. The slides were identified and quantified by counting the number of cells per field, the number of infected cells, and the number of amastigotes per cell using light microscopy.

### **3.5 Synergism Calculations**

To assess the synergistic effects of the drug combinations in this study, we employed a combination of statistical and mathematical models to provide insights into the interactions between the drugs and their effectiveness against *T. cruzi* amastigotes.

#### **3.5.1 Two-way ANOVA**

A two-way ANOVA was conducted to evaluate the main effects of two independent variables on the reduction of *T. cruzi* amastigotes per cell. This method allowed us to examine whether drug type and concentration individually have significant effects and whether their interaction produces a different outcome than expected. To analyze the data, we partitioned the total variability, expressed as Sum of Squares, into components: variability due to drug type, concentration, and their interaction, along with unexplained variability (residual). Degrees of freedom were assigned to each component based on the number of groups and observations. Mean squares were obtained by dividing each sum of squares by the corresponding degrees of freedom, and F-statistics were computed as the ratio of mean squares of the factors to the mean square of the residual. Finally, p-values were calculated from the F-statistics, where values smaller than 0.05 indicate statistically significant effects, meaning that we can reject the null

hypothesis and conclude that the factor or interaction has a meaningful impact on the outcome (41).

### **3.5.2 Bliss Independence Model**

We applied the Bliss Independence Model to predict the expected effect of the drug combinations, assuming that the drugs act independently and through different mechanisms of action. By comparing the observed effects to the predicted outcomes, we identified potential synergy when the observed results exceeded the expected values. This model provided deeper insight into the synergy between the drugs.

### **3.5.3 Fractional Inhibitory Concentration Index**

To quantify the combined effect of Ilmofoosine and Ketoconazole, we employed the Fractional Inhibitory Concentration Index based on Loewe's additivity model. The combinatory effect was determined using Eq1 and interpreted according to the criteria set by Loewe's model, where a FICI of 1 denotes an additive effect. A FICI below 1 indicates a synergistic effect, whereas above 1 signifies antagonism (44–46). This implies that a smaller or larger amount of the drug is needed to achieve the same effect as when the drugs are used individually.

## **3.6 Molecular Modeling**

### **3.6.1 Ligand Preparation**

Initially, we utilized Avogadro software to 3D model ilmofoosine and ketoconazole, based on their 2D structures obtained from PubChem under the codes PubChem CID 55008 for ilmofoosine and PubChem CID 47576 for ketoconazole. This sophisticated molecular editor and visualizer is designed for computational chemistry across various platforms. Avogadro features flexible, high-resolution rendering capabilities and supports a robust plugin architecture. Next, we used AutoDockTools to prepare these drugs for docking by merging non-polar hydrogens and adding Gasteiger charges to simulate the electrostatic interactions with accuracy (56,57).

### **3.6.2 Protein Preparation**

We utilized the AlphaFold protein structure database, an AI system developed by Google DeepMind that predicts a protein's 3D structure from its amino acid sequence with high accuracy. The structures obtained were: Phosphatidylethanolamine N-methyltransferase from Homo sapiens (code AF-Q9UBM1-F1), Sterol 14-alpha demethylase in *T. cruzi* (code AF-Q7Z1V1-F1), and Sterol 24-C-methyltransferase from *T. cruzi* (code AF-Q9UBM1-F1). Using AutoDockTools, we added polar hydrogens, merged non-polar hydrogens, added Kollman charges, deleted water molecules, and assigned AD4 atom types. Assigning AD4 types and Kollman charges ensures accurate electrostatic interactions and proper atom type identification during the docking process (58).

### **3.6.3 Grid**

A blind docking approach was utilized, where the grid box covered the entire surface of the protein to predict the ligand's binding site. We ran AutoGrid with a nice level of 0, which prioritizes the docking process to run with maximum CPU usage, ensuring faster and more efficient computations (58).

### **3.6.4 Docking Simulation**

For docking, we configured the protein as a rigid structure while allowing the ligand to remain flexible. We opted for the long genetic algorithm setting to increase the number of generations and evaluations, thereby enhancing the likelihood of identifying the optimal binding conformation. The Lamarckian Genetic Algorithm (GA) combines genetic search methods with local search optimization, improving the docking accuracy by refining ligand poses (56). Finally, we ran AutoDock with a nice level of 0 to utilize maximum computational resources.

### **3.6.5 Analysis**

To analyze the results, we displayed the obtained conformations ranked by binding energy and built the hydrogen bonds.



## 4. Results and Discussion

### 4.1 Experimental Evidence of Synergy

In this study, we investigated the impact of varying concentrations of ilmofosine on the replication of *Trypanosoma cruzi* amastigotes in Vero cell cultures (Figure 6). At an initial concentration of 0.4  $\mu\text{M}$ , we observed a noticeable reduction in the number of amastigotes, indicating an inhibitory effect on parasite replication. Increasing the concentration to 0.6  $\mu\text{M}$  resulted in a further decline in amastigote numbers, demonstrating a dose-dependent response. At a concentration of 0.8  $\mu\text{M}$ , there was a marked suppression of *T. cruzi* amastigote replication, with only a few parasites detected. When the concentration was increased to 1  $\mu\text{M}$ , *T. cruzi* amastigotes were entirely eradicated from the cell cultures. These findings underscore the significant efficacy of ilmofosine in a concentration-dependent manner, highlighting its potential as a promising therapeutic agent against *T. cruzi* infections.

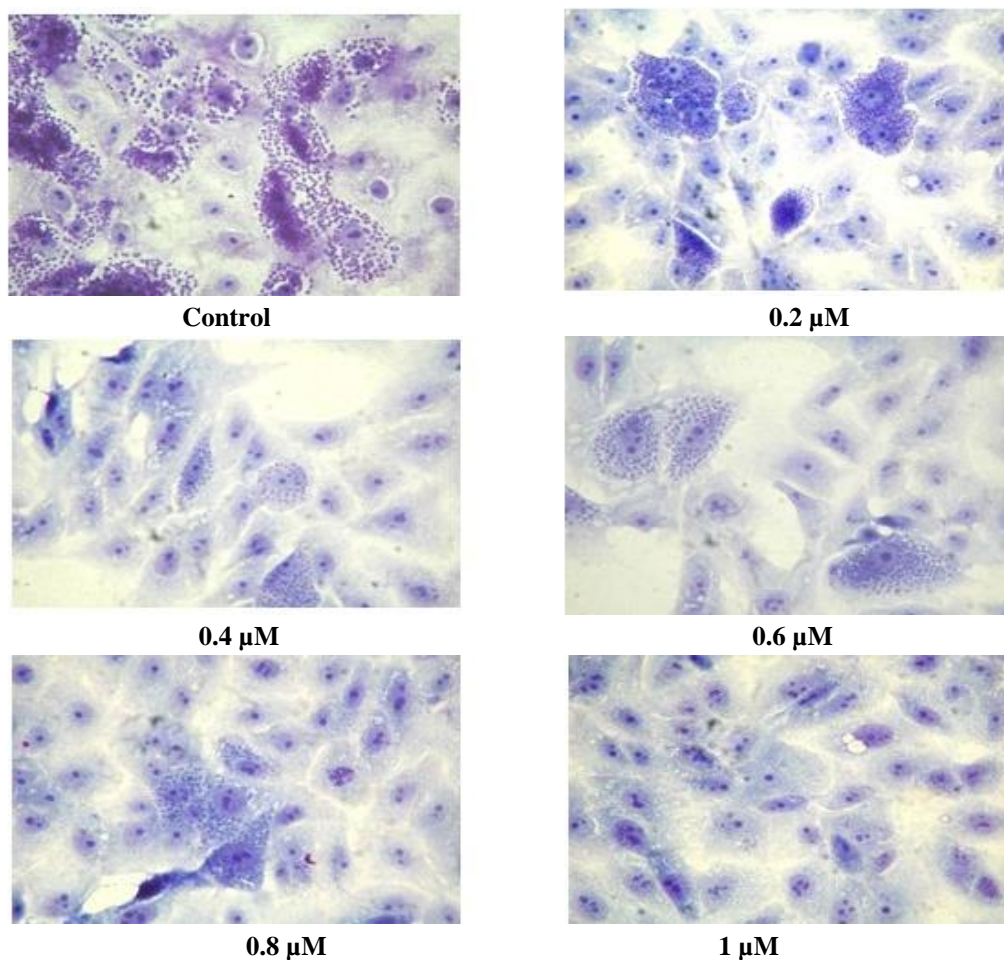


Figure 6: Impact of different concentrations of Ilmofosine on the replication of *T. cruzi* amastigotes in Vero cell cultures. Own authorship.

Similarly, we evaluated the effect of different concentrations of ketoconazole on the replication of *Trypanosoma cruzi* amastigotes in Vero cell cultures (Figure 7). At 1 nM, a reduction in amastigote numbers was observed, indicating the drug's inhibitory impact. Increasing the concentration to 2 nM further decreased the amastigote count, confirming a dose-dependent response. At 3 nM, the replication of *T. cruzi* amastigotes was significantly hindered, with only a few parasites remaining. Finally, at a concentration of 4 nM, the amastigotes were completely eradicated from the cell cultures. These findings demonstrate the potent efficacy of ketoconazole in a concentration-dependent manner, underscoring its potential as a therapeutic agent against *T. cruzi* infections.

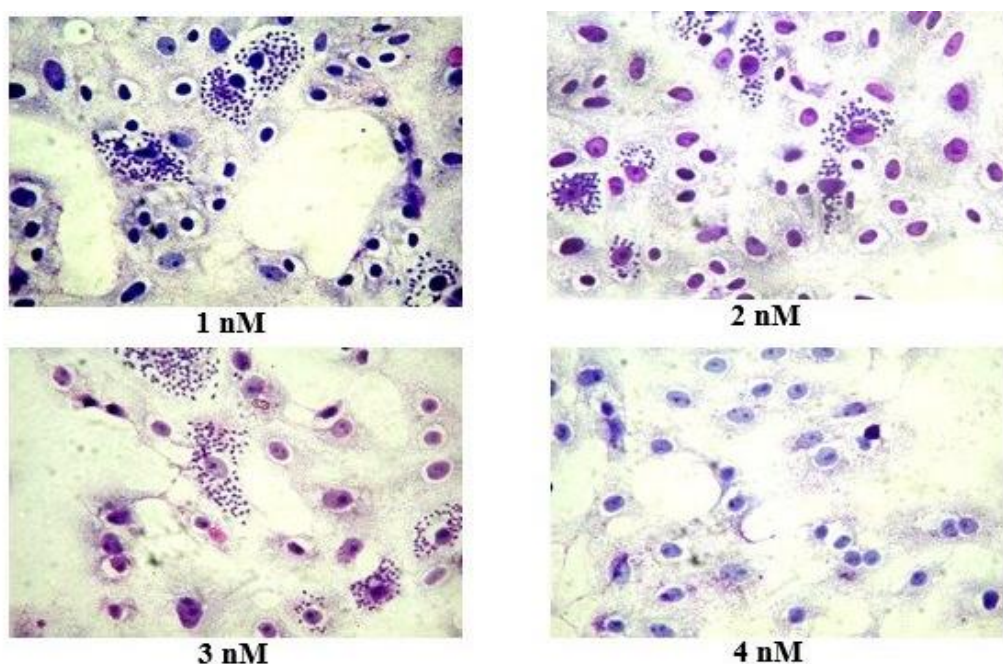


Figure 7: Impact of different concentrations of Ketoconazole on the replication of *T. cruzi* amastigotes in Vero cell cultures. Own authorship.

Next, we evaluated the synergistic and combined effect of ilmofosine and ketoconazole on the replication of *Trypanosoma cruzi* amastigotes in Vero cell cultures (Figure 8). The combination of ilmofosine at 0.2  $\mu$ M with ketoconazole at 1 nM resulted in a notable reduction in amastigote numbers, suggesting an enhanced inhibitory effect compared to the individual treatments. Increasing the concentration of ilmofosine to 0.4  $\mu$ M while keeping ketoconazole at 1 nM further decreased the amastigote count. Additionally, the combination of ilmofosine at 0.2  $\mu$ M with ketoconazole at 2 nM significantly eradicated amastigote replication, demonstrating a synergistic interaction. Finally, the combination of ilmofosine at 0.4  $\mu$ M with ketoconazole at 2 nM was performed to corroborate that higher concentrations also result in complete eradication of amastigotes from the cell cultures. These results highlight the potential of combining ilmofosine and ketoconazole as a more effective treatment strategy against *T. cruzi* infections.

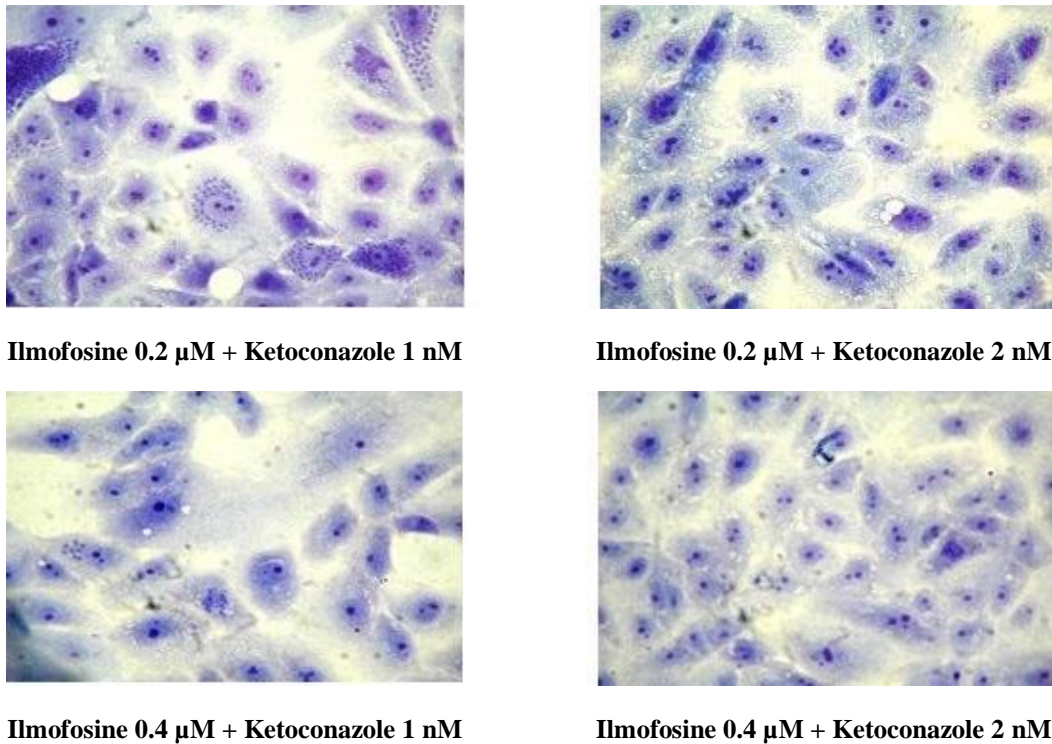


Figure 8: Synergistic effect of Ilmofosine and Ketoconazole on the replication of *T. cruzi* amastigotes in Vero cell cultures. Own authorship.

After evaluating the synergistic effects of Ilmofosine and Ketoconazole on the replication of *T. cruzi* amastigotes in Vero cell cultures, we generated dose-response curves for ilmofosine (Fig. 9), ketoconazole (Fig. 10), and the combination of ketoconazole at 2 nM with ilmofosine (Fig. 11). These curves provided a clearer visualization of the percentage of inhibition relative to drug concentration, allowing us to identify the MIC for each drug when used alone and in combination to eradicate amastigotes in Vero cell cultures.

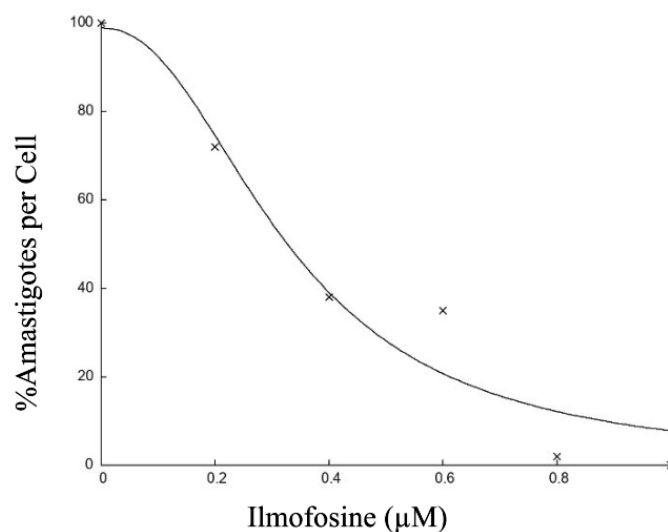


Figure 9: Dose-response curve of Ilmofosine on the replication of *T. cruzi* amastigotes per cell. Own authorship.

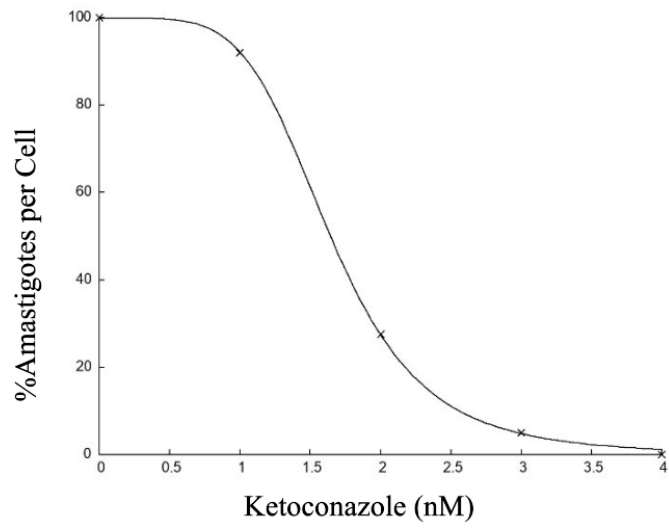


Figure 10: Dose-response curve of ketoconazole on the replication of *T. cruzi* amastigotes per cell. Own authorship.

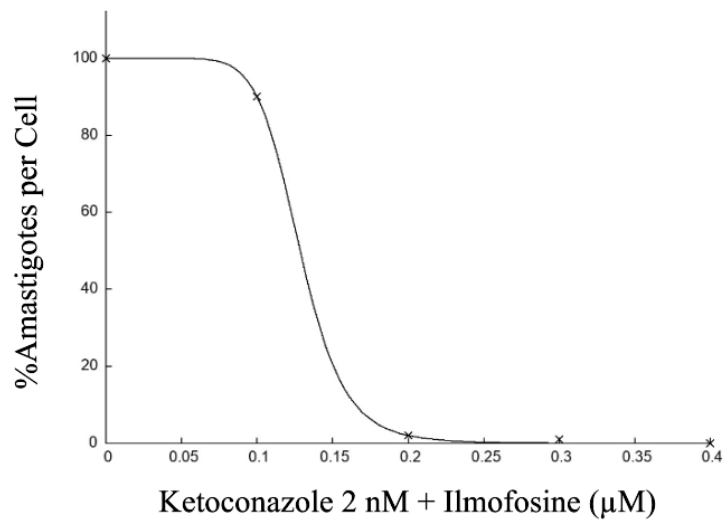


Figure 11: Dose-response curve of Ketoconazole at 2 nM combined with Ilmofosine on the replication of *T. cruzi* amastigotes per cell. Own authorship.

## 4.2 Two-way ANOVA

Once we analyzed the data from the effects of Ilmofosine and Ketoconazole on the replication of *T. cruzi* amastigotes in Vero cell cultures and generating the dose-response curves, we used this data to perform a two-way ANOVA. The results are presented in the following table:

**Table 1. Two-way ANOVA analysis of drug type, concentration, and their interaction effects on *T. cruzi* amastigote replication**

Factor	Sum of Squares	Degrees of Freedom	Mean Square	F-statistic	p-value
Drug Type	1386.67	2	693.33	1166.35	$1.43 \times 10^{-25}$
Concentration	43250.21	10	4325.02	7275.74	$5.17 \times 10^{-43}$
Interaction	143468.54	20	7173.43	12067.45	$7.54 \times 10^{-51}$
Residual (Error)	17.83	30	0.59		

The results of the two-way ANOVA observed in Table 1 indicate significant effects for all factors examined. The p-value for drug type is  $1.43 \times 10^{-25}$ , which is far smaller than the threshold of 0.05. This leads us to reject the null hypothesis that drug type has no effect on the outcome. Therefore, drug type has a statistically significant influence on the reduction of amastigotes per cell.

Similarly, the p-value for concentration is  $5.17 \times 10^{-43}$ , again much lower than 0.05, allowing us to reject the null hypothesis that concentration has no effect on the outcome. This suggests that the concentration of the drugs plays a critical role in determining the extent of amastigote reduction.

Lastly, the interaction between drug type and concentration shows a p-value of  $7.54 \times 10^{-51}$ , also significantly below 0.05. As a result, we reject the null hypothesis that there is no interaction between these two factors. This confirms that the combination of drug type and concentration leads to a substantially different effect than would be expected from their individual actions.

Overall, both drug type and concentration, as well as their interaction, significantly affect the reduction of amastigotes, providing strong evidence that Ilmofosine and Ketoconazole, when combined, work more effectively than when used alone. This supports the hypothesis that the drugs act synergistically, likely due to their different mechanisms of action.

## 4.3 Bliss Independence Model

Following the two-way ANOVA, we applied the Bliss Independence Model to further investigate the interactions between Ilmofosine and Ketoconazole. This model operates on the assumption that the drugs act independently, we were able to predict the expected combined effect based on their individual effects by using Equation 1:

$$E_{AB} = E_A + E_B - (E_A \times E_B)$$

Here,  $E_A$  represents the effect of ilmofosine alone,  $E_B$  the effect of ketoconazole alone and  $E_{AB}$  the expected effect of the drug combination. Considering that the best observed inhibition was 98% when we used the combination of ilmofosine at 0.2  $\mu$ M and ketoconazole at 2 nM, we used the inhibition percentages for Ilmofosine alone at 0.2  $\mu$ M and Ketoconazole alone at 2 nM. By substituting these individual effects into the equation, we obtained the following results:

$$E_{AB} = 0.28 + 0.75 - (0.28 \times 0.75) = 0.82 = 82\%$$

By comparing this expected inhibition of 82% to the observed inhibition of 98%, we can notice that the observed inhibition is greater than the expected, thus the drugs do not act entirely independently suggesting that the interaction is synergistic. Specifically, the combination at lower concentrations showed a marked increase in inhibition compared to either drug alone, indicating that they may enhance each other's efficacy in the treatment of *T. cruzi* amastigotes.

#### 4.4 Fractional Inhibitory Concentration Index

Subsequently, we used the FICI equation (Eq 2) to quantify the degree of interaction and synergistic effect between the drugs:

$$FICI = FIC_A + FIC_B = \frac{C_A}{MIC_A} + \frac{C_B}{MIC_B}$$

Here,  $C_A$  represents the concentration of ilmofosine when used in combination with ketoconazole that is effective at inhibiting the parasite growth,  $MIC_A$  indicates the lowest concentration of ilmofosine used alone to inhibit the visible growth of the parasite. Analogously applies for B, which stands for ketoconazole.

$$FICI = \frac{0.2\mu M}{1\mu M} + \frac{2nM}{4nM} = 0.7$$

According to the literature, a FICI value of 0.7 indicates a synergistic effect, suggesting that the combination of ilmofosine and ketoconazole enhances the inhibitory effect against *T. cruzi* amastigotes compared to each drug used individually. To further illustrate this synergistic interaction, we constructed an isobologram based on Loewe's Additivity model (Figure 12). Our isobologram showed that the combination point of ilmofosine and ketoconazole fell below the additive isobole, reaffirming the synergistic interaction ( $FICI < 1$ ). This indicates that lower doses of each drug are needed in combination to achieve the same effect as higher doses of the drugs used alone. This synergistic effect not only enhances the therapeutic efficacy but also potentially reduces the side effects associated with higher doses of individual drugs. Therefore, our study highlights the potential benefits of using a combination therapy of ilmofosine and ketoconazole for the treatment of Chagas disease, offering a promising approach to improve patient outcomes.

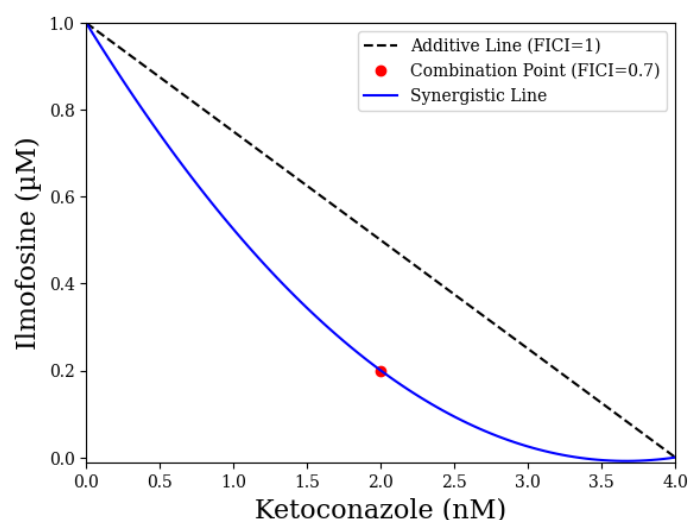


Figure 12: Isobologram curve describing the synergistic effect of Ilmofosine and Ketoconazole on *T. cruzi* amastigotes replication. Own authorship.

#### 4.5 Comparative Docking Studies of Ilmofosine and Ketoconazole

Once the synergistic effect between Ilmofosine and Ketoconazole had been mathematically and graphically verified, we proceeded to examine the interactions between these drugs and the target enzymes of sterol 14 $\alpha$ -demethylase and sterol 24-C-methyltransferase on ergosterol biosynthesis pathway and PEMT on Bremer-Greenberg transmethylation pathway through molecular modeling and docking simulations. Initially, a docking simulation of each drug/ligand was conducted with each enzyme/protein separately, resulting in the following tables and figures.

**Table 2. Interaction Analysis of Ilmofosine and Phosphatidylethanolamine N-methyltransferase from *Homo sapiens***

Conformations	1	2	3	4	5
Binding Energy (kcal/mol)	-4.15	-2.43	-1.97	-1.89	-1.24
Intermolecular Energy (kcal/mol)	-11.1	-10.18	-9.73	-9.65	-9
Hydrogen Bonds	Arg67	Lys38	Asn64	Lys38	
Distance (Å)	2.161	1.92	2.084	1.808	

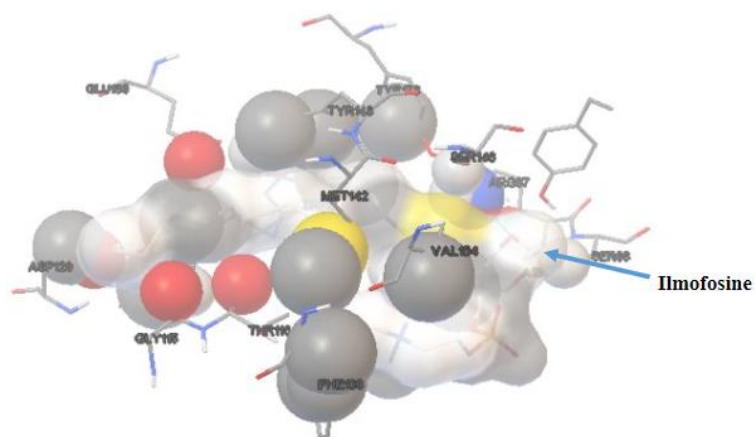


Figure 13: Most likely binding position of Ilmofosine and Phosphatidylethanolamine N-methyltransferase from Homo sapiens. Own authorship.

**Table 3. Interaction Analysis of Ketoconazole and Phosphatidylethanolamine N-methyltransferase from Homo sapiens**

Conformations	1	2	3	4	5
Binding Energy (kcal/mol)	-9.7	-8.67	-7.81	-7.7	-7.61
Intermolecular Energy (kcal/mol)	-11.78	-10.76	-9.89	-9.79	-9.7
Hydrogen Bonds					Asn64
Distance (Å)					2.103

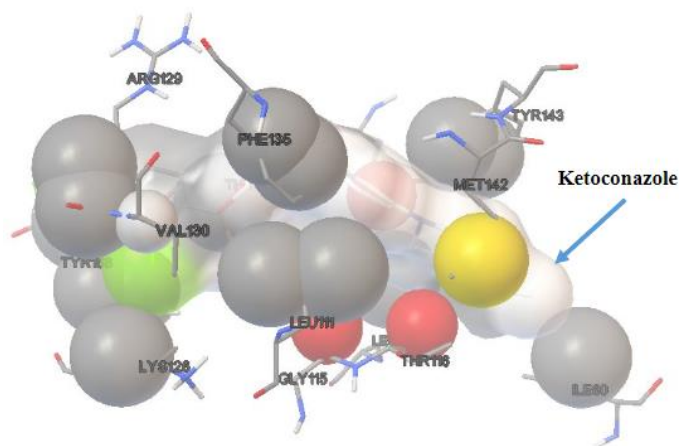
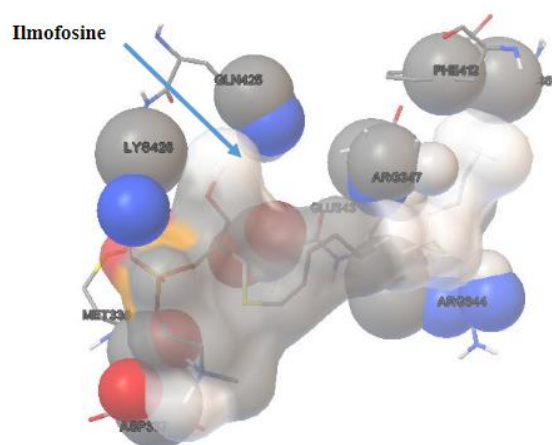


Figure 14: Most likely binding position of Ketoconazole and Phosphatidylethanolamine N-methyltransferase from Homo sapiens. Own authorship.



**Table 4. Interaction Analysis of Ilmofosine and Sterol 14 $\alpha$ -demethylase from *T. cruzi***

Conformations	1	2	3	4	5
Binding Energy (kcal/mol)	-2.38	-2.22	-2.06	-2.02	-1.41
Intermolecular Energy (kcal/mol)	-10.13	-9.98	-9.82	-9.78	-9.17
Hydrogen Bonds	Lys426	Tyr116			Gln199
Distance (Å)	1.861	1.831			1.913

Figure 15: Most likely binding position of Ilmofosine and Sterol 14 $\alpha$ -demethylase from *T. cruzi*. Own authorship.**Table 5. Interaction Analysis of Ketoconazole and Sterol 14 $\alpha$ -demethylase from *T. cruzi***

Conformations	1	2	3	4	5
Binding Energy (kcal/mol)	-8.38	-8.27	-8.05	-7.97	-7.9
Intermolecular Energy (kcal/mol)	-10.47	-10.36	-10.14	-10.06	-9.99
Hydrogen Bonds	Tyr103	Leu357		Met358	Tyr103
Distance (Å)	2.187	2.053		2.029	1.92

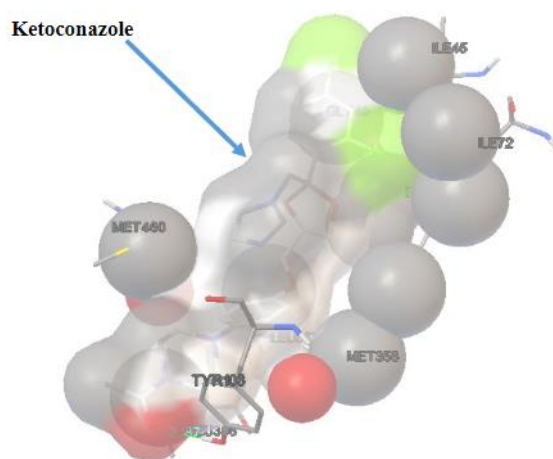


Figure 16: Most likely binding position of Ketoconazole and Sterol 14 $\alpha$ -demethylase from *T. cruzi*. Own authorship.

**Table 6. Interaction Analysis of Ilmofosine and Sterol 24-C-methyltransferase from *T. cruzi***

Conformations	1	2	3	4	5
Binding Energy (kcal/mol)	-4.99	-3.17	-2.76	-2.2	-2.13
Intermolecular Energy (kcal/mol)	-12.75	-10.92	-10.51	-9.96	-9.88
Hydrogen Bonds	Phe95	Leu97			
Distance (Å)	1.975	1.768			

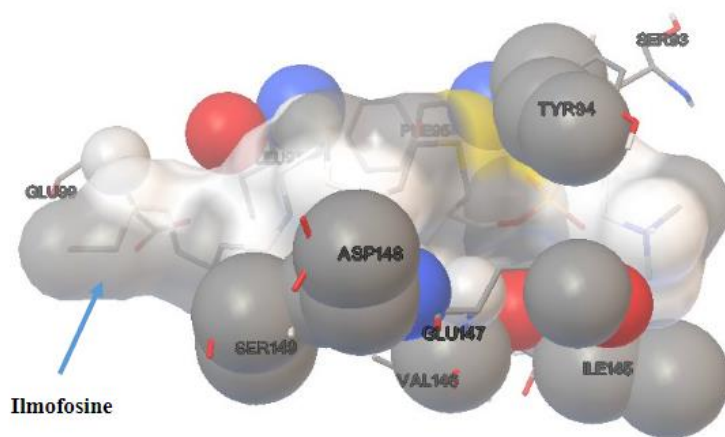


Figure 17: Most likely binding position of Ilmofosine and Sterol 24-C-methyltransferase from *T. cruzi*. Own authorship.

**Table 7. Interaction Analysis of Ketoconazole and Sterol 24-C-methyltransferase from *T. cruzi***

Conformations	1	2	3	4	5
Binding Energy (kcal/mol)	-11.53	-11.31	-10.48	-10.37	-9.77
Intermolecular Energy (kcal/mol)	-13.61	-13.4	-12.57	-12.46	-11.86
Hydrogen Bonds	Phe95	Val152	Leu97	Leu97	Cys101
Distance (Å)	2.222	1.98	1.798	2.036	2.234
Hydrogen Bonds	Glu99	Glu147	Gly92	Gly92	Glu147
Distance (Å)	2.149	2.034	2.2	1.844	2.181

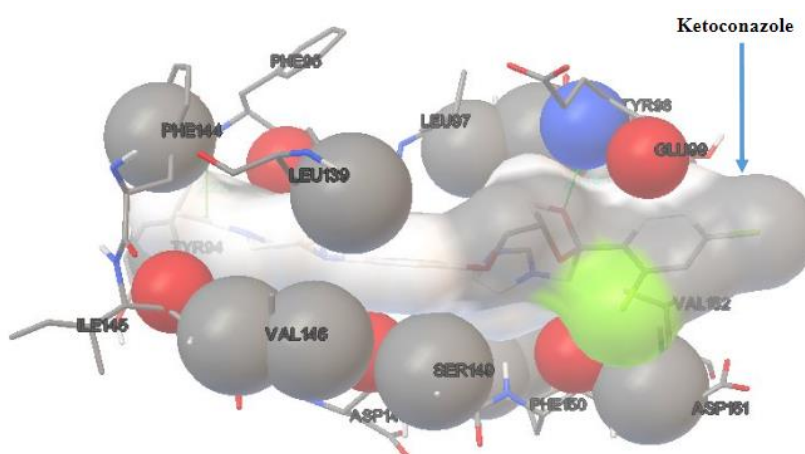


Figure 18: Most likely binding position of Ketoconazole and Sterol 24-C-methyltransferase from *T. cruzi*. Own authorship.

The binding between ilmofosine and PEMT has a relatively high intermolecular energy of -11.1 kcal/mol (Table 2), involving van der Waals forces, hydrogen bond energy, and electrostatic energy. These components contribute significantly to the stability of the complex. Although the binding energy is not extremely strong, the interaction energies highlight the importance of non-covalent interactions in the binding process. These non-covalent interactions play a crucial role in stabilizing the complex and facilitating the binding between ilmofosine and PEMT.

The binding between ketoconazole and PEMT demonstrates a notable interaction, evidenced by a strong binding energy of -9.7 kcal/mol and a relatively high intermolecular energy of -11.78 kcal/mol (Table 3), which indicates a stable complex formation. These robust interactions suggest that ketoconazole has a strong affinity for PEMT, highlighting its surprising potential as an effective inhibitor. It is important to note that PEMT has not been extensively studied using docking simulations, resulting in limited literature with reference values. However, one study involving PEMT and epigallocatechin 3-gallate reported a docking result with a binding energy of -7 kcal/mol, which is considered an ideal binding energy for protein-ligand interactions. This makes our results promising for further investigations (59).

The results obtained from the binding of ilmofosine and Sterol 14 $\alpha$ -demethylase indicate relatively weak interactions, as evidenced by a low binding energy of -2.38 kcal/mol and a slightly strong intermolecular energy of -10.13 kcal/mol (Table 4). Despite the presence of interactions and numerous hydrogen bonds, these values suggest that the binding affinity is insufficiently strong. Thus, while ilmofosine does form interactions with Sterol 14 $\alpha$ -demethylase, its potential as an effective inhibitor remains questionable due to the relatively weak binding energies observed.

The binding analysis of ketoconazole with Sterol 14 $\alpha$ -demethylase demonstrates strong interactions across various conformations. The binding energies range from -8.38 to -7.9 kcal/mol, indicating relatively strong binding. The slightly strong intermolecular energies ranging from -10.47 to -9.99 kcal/mol (Table 5), highlight significant contributions from van der Waals forces and hydrogen bonds. These interactions suggest that ketoconazole has a stable and effective binding affinity for Sterol 14 $\alpha$ -demethylase, supporting its inhibitory action. Rojas et al. (2019) also performed docking studies between ketoconazole and Sterol 14 $\alpha$ -demethylase, reporting a binding energy of -10.29 kcal/mol, which aligns closely with the binding energies observed in our study. Furthermore, their study identified key binding site residues such as Met358, Met460, Leu357, and Tyr103, which were also observed in our results, further validating the consistency of these interactions (60).

The interaction analysis of Ilmofosine with Sterol 24-C-methyltransferase shows a moderate affinity, with a binding energy of -4.99 kcal/mol. The intermolecular energy of -12.75 kcal/mol (Table 6) indicates substantial stabilization, driven by non-covalent interactions such as van der Waals forces and electrostatic interactions. The presence of strong hydrogen bonds further enhances the stability and specificity of the Ilmofosine-enzyme complex. These results suggest that Ilmofosine could effectively bind to and inhibit Sterol 24-C-methyltransferase, positioning it as a promising therapeutic agent against Chagas disease. Similar docking studies have been performed with Sterol 24-C-methyltransferase and miltefosine, another alkyl-lysophospholipid from the same family as Ilmofosine, yielding a comparable binding energy of -4 kcal/mol (53). These results suggest that Ilmofosine could effectively bind to and inhibit Sterol 24-C-methyltransferase, positioning it as a promising therapeutic agent against Chagas disease.

The interaction analysis of ketoconazole with Sterol 24-C-methyltransferase reveals a high binding affinity, with a binding energy of -11.53 kcal/mol. The intermolecular energy of -13.61 kcal/mol (Table 7) points to significant stabilization from non-covalent interactions. Notably, multiple hydrogen bonds, particularly with Phe95 and Glu99, contribute to the strong binding and specificity of the ketoconazole-enzyme complex. This robust binding suggests that ketoconazole effectively interacts with and potentially inhibits Sterol 24-C-methyltransferase, highlighting its potential utility in therapeutic applications against Chagas disease. Although azasterols are considered the primary inhibitors of Sterol 24-C-methyltransferase, with binding energies around -7.6 kcal/mol, it has been demonstrated that 24SMT is also sensitive to inhibition by azole drugs such as ketoconazole, supported by the higher binding energy found in docking studies, exceeding the binding strength of azasterols (53,61). This robust binding suggests that ketoconazole effectively interacts with and potentially inhibits Sterol 24-C-

methyltransferase, highlighting its potential utility in therapeutic applications against Chagas disease.

#### 4.6 Docking Studies of Both Drugs at the Same Time: Searching for Synergy

In this study, we employed a novel docking approach by simultaneously investigating the interaction of both drugs with the target enzymes, an advanced method that allows us to explore potential synergies between the compounds. Unlike traditional docking studies, which evaluate individual ligands in isolation, our method identified and selected the binding sites with the highest affinity for each drug within the enzymes. Additionally, we focused on regions where both ligands could potentially share hydrogen bonds, creating a protein/ligand complex. This innovative approach enabled us to perform a combined docking simulation, allowing for an in-depth analysis of how each ligand interacts with the enzyme in the presence of the other. This strategy offers valuable insights into how the two drugs may complement each other, potentially enhancing their inhibitory effects. The results of these interactions are presented in the tables and figures below

**Table 8. Interaction Analysis of Ilmofosine and Phosphatidylethanolamine N-methyltransferase from Homo sapiens with Ketoconazole bound in its most likely position**

Conformations	1	2	3	4	5
Binding Energy (kcal/mol)	-4.38	-2.89	-1.85	-1.49	-1
Intermolecular Energy (kcal/mol)	-11.14	-9.95	-9.61	-9.24	-8.76
Hydrogen Bonds			Ser68		Thr72
Distance (Å)			1.746		1.876

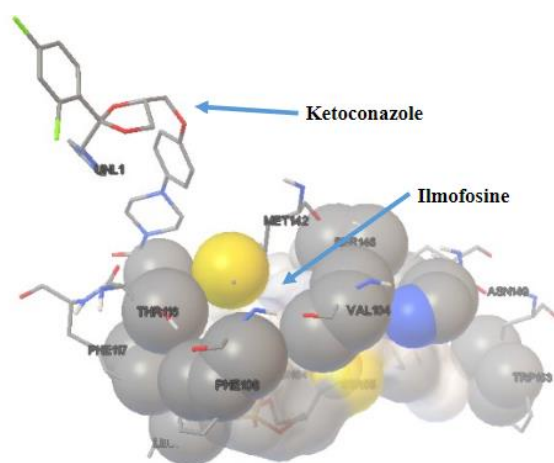


Figure 19: Strongest interaction of Ilmofosine and Phosphatidylethanolamine N-methyltransferase from Homo sapiens with Ketoconazole bound in its most likely position. Own authorship.

**Table 9. Interaction Analysis of Ilmofosine and Phosphatidylethanolamine N-methyltransferase from Homo sapiens with Ketoconazole bound in Asn64**

Conformations	1	2	3	4	5
Binding Energy (kcal/mol)	-3.97	-2.41	-1.09	-0.59	-0.51
Intermolecular Energy (kcal/mol)	-10.72	-9.86	-8.84	-8.34	-8.26
Hydrogen Bonds		Thr72			Lys126
Distance (Å)		1.895			2

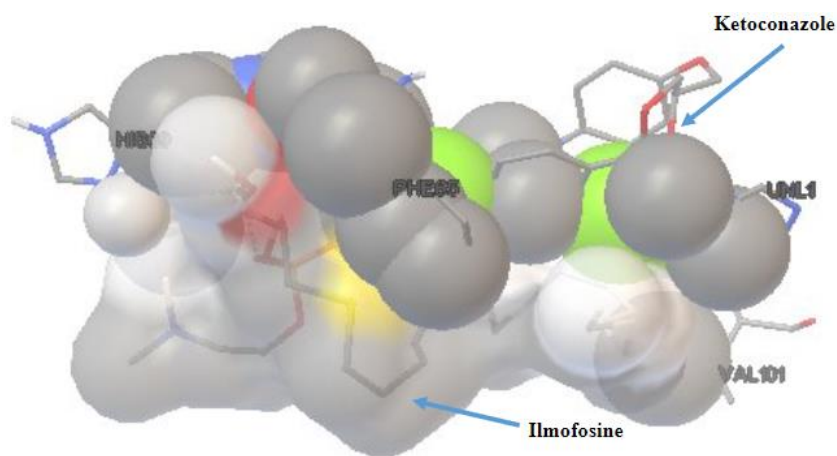


Figure 20: Strongest interaction of Ilmofosine and Phosphatidylethanolamine N-methyltransferase from Homo sapiens with Ketoconazole bound to a common Hydrogen Bond site. Own authorship.

**Table 10. Interaction Analysis of Ketoconazole and Phosphatidylethanolamine N-methyltransferase from Homo sapiens with Ilmofosine bound in its most likely position**

Conformations	1	2	3	4	5
Binding Energy (kcal/mol)	-8.85	-8	-7.43	-7.11	-6.54
Intermolecular Energy (kcal/mol)	-10.93	-10.09	-9.52	-9.2	-8.63
Hydrogen Bonds	Val130	His69	Arg34	Lys38	
Distance (Å)	2.1	1.992	1.937	1.984	

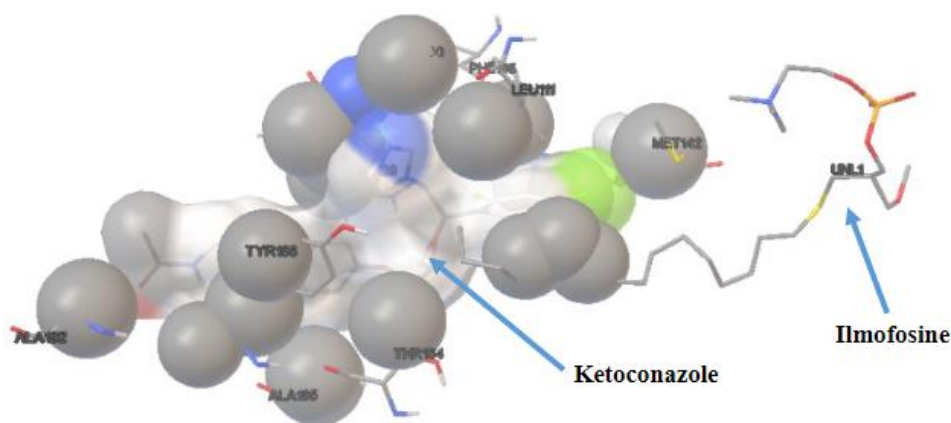


Figure 21: Strongest interaction of Ketoconazole and Phosphatidylethanolamine N-methyltransferase from Homo sapiens with Ilmofosine bound in its most likely position. Own authorship.

**Table 11. Interaction Analysis of Ketoconazole and Phosphatidylethanolamine N-methyltransferase from Homo sapiens with Ilmofosine bound in Asn64**

Conformations	1	2	3	4	5
Binding Energy (kcal/mol)	-8.3	-8.04	-7.41	-7.24	-7.11
Intermolecular Energy (kcal/mol)	-10.39	-10.13	-9.5	-9.33	-9.2
Hydrogen Bonds		Val130			
Distance (Å)		1.958			

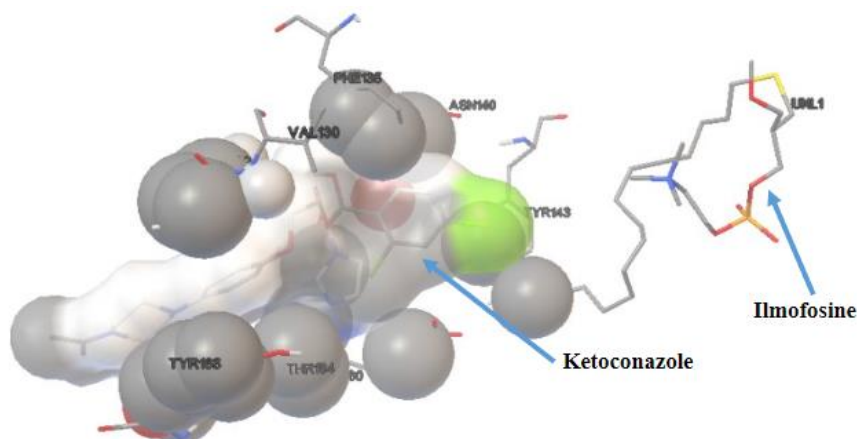


Figure 22: Strongest interaction of Ketoconazole and Phosphatidylethanolamine N-methyltransferase from Homo sapiens with Ilmofosine bound to a common Hydrogen Bond site. Own authorship.

When comparing the interaction analysis of ilmofosine with PEMT in the presence of ketoconazole (Tables 8 and 9), we observe that the strongest interactions between ilmofosine and the enzyme complex occur when ilmofosine binds near the site where ketoconazole is already bound (Figures 19 and 20). Notably, Table 8 shows that the binding and intermolecular energies of ilmofosine are stronger in the presence of ketoconazole,

suggesting that their interactions within similar regions of the enzyme, due to their proximity, lead to an enhanced inhibitory effect (synergy) when used together. This indicates that the presence of one drug can potentially enhance or stabilize the binding of the other. This phenomenon, known as cooperative or synergistic binding, occurs when two drugs bind near each other and decrease the likelihood of either drug dissociating from the enzyme, resulting in a prolonged duration of inhibition as the enzyme remains occupied for a longer period (62,63).

On the other hand, a slightly weaker binding and intermolecular energy is observed in Tables 10 and 11 when ilmofosine first forms a complex with PEMT and ketoconazole subsequently binds near it (Figures 21 and 22). However, this does not imply that the drugs are antagonistic. Generally, the binding affinity of any drug may decrease when two ligands bind in close proximity due to steric hindrance or altered binding site dynamics. When two drugs bind very close to the same site on an enzyme and maintain nearly the same binding energy with only a slight reduction, it indicates that the drugs can coexist in the binding pocket without significantly interfering with each other's interactions. The individual affinities of the drugs and the conformational flexibility of the enzyme likely contribute to this stability, allowing both drugs to effectively bind and exert their therapeutic effects even in close proximity (62).

**Table 12. Interaction Analysis of Ilmofosine and Sterol 14 $\alpha$ -demethylase from *T. cruzi* with Ketoconazole bound in Tyr103**

Conformations	1	2	3	4	5
Binding Energy (kcal/mol)	-1.81	-0.69	-0.21	-0.21	-0.07
Intermolecular Energy (kcal/mol)	-9.56	-8.44	-7.96	-7.96	-7.83
Hydrogen Bonds	Gln293	Arg230	Ala211	Lys376	
Distance (Å)	1.826	2.08	1.838	2.139	

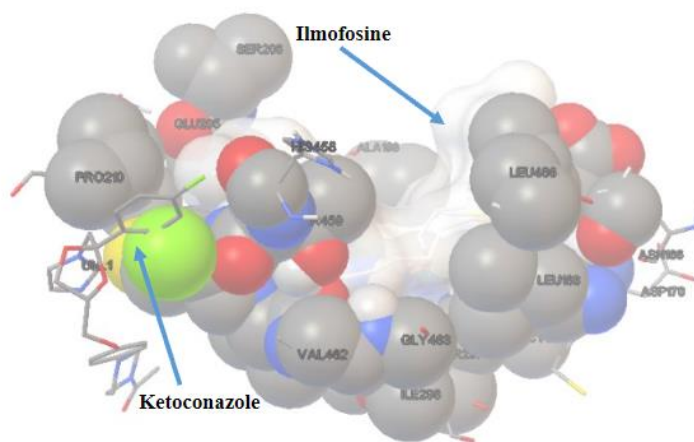


Figure 23: Strongest interaction of Ilmofosine and Sterol 14 $\alpha$ -demethylase from *T. cruzi* with Ketoconazole bound in its most likely position. Own authorship.



**Table 13. Interaction Analysis of Ilmofosine and Sterol 14 $\alpha$ -demethylase from *T. cruzi* with Ketoconazole bound in Leu357**

Conformations	1	2	3	4	5
Binding Energy (kcal/mol)	-1.65	-1.36	-0.44	-0.26	0.51
Intermolecular Energy (kcal/mol)	-9.41	-9.12	-8.2	-8.02	-7.25
Hydrogen Bonds					Ser202
Distance (Å)					2.751

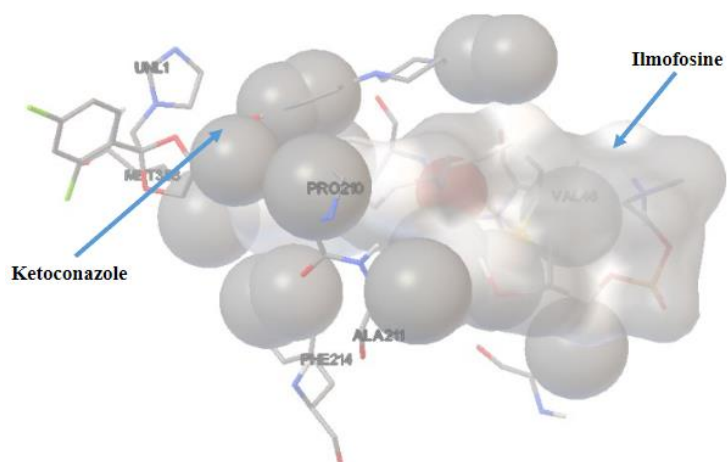


Figure 24: Strongest interaction of Ilmofosine and Sterol 14 $\alpha$ -demethylase from *T. cruzi* with Ketoconazole bound in its second most likely position. Own authorship.

**Table 14. Interaction Analysis of Ketoconazole and Sterol 14 $\alpha$ -demethylase from *T. cruzi* with Ilmofosine bound in Lys426**

Conformations	1	2	3	4	5
Binding Energy (kcal/mol)	-8.46	-7.77	-7.49	-7.44	-7.22
Intermolecular Energy (kcal/mol)	-10.54	-9.86	-9.57	-9.53	-9.31
Hydrogen Bonds	Leu357	Thr459	Met358		
Distance (Å)	1.898	2.989	2.002		

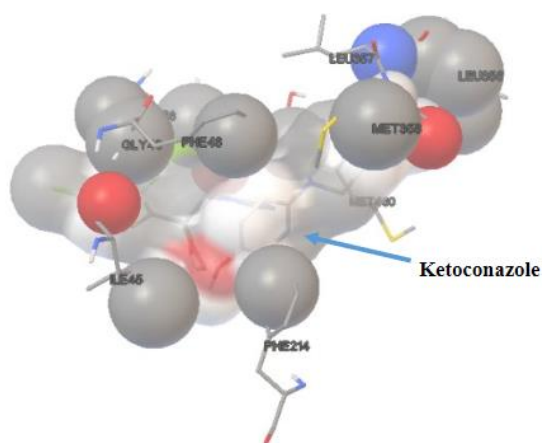


Figure 25: Strongest interaction of Ketoconazole and Sterol 14 $\alpha$ -demethylase from *T. cruzi* with Ilmofosine bound in its most likely position. Own authorship.

**Table 15. Interaction Analysis of Ketoconazole and Sterol 14 $\alpha$ -demethylase from *T. cruzi* with Ilmofosine bound in Tyr116**

Conformations	1	2	3	4	5
Binding Energy (kcal/mol)	-8.21	-6.86	-6	-5.58	-5.58
Intermolecular Energy (kcal/mol)	-10.3	-8.95	-8.09	-7.67	-7.67
Hydrogen Bonds			Arg228	Ala211	His458
Distance (Å)			2.038	2.106	2.13
Hydrogen Bonds				Gln225	
Distance (Å)				1.864	

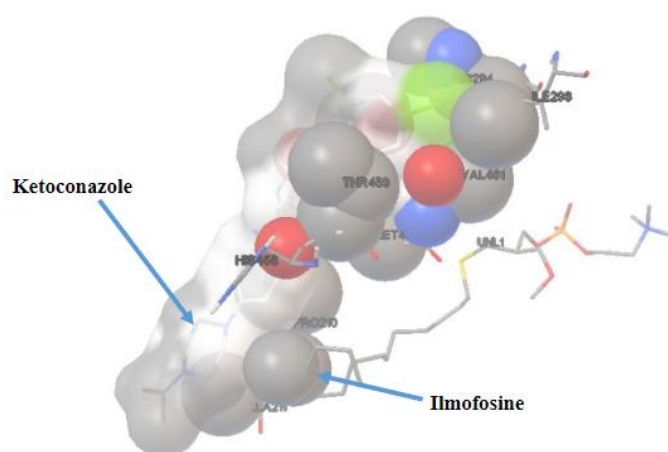


Figure 26: Strongest interaction of Ketoconazole and Sterol 14 $\alpha$ -demethylase from *T. cruzi* with Ilmofosine bound in its second most likely position. Own authorship.

As expected from the results in Table 3, the interactions of ilmofosine with sterol 14 $\alpha$ -demethylase in the presence of ketoconazole (Tables 12 and 13) are weaker than previously

observed. Both the binding energy and intermolecular energy have decreased. Although ilmofosine binds relatively close to the site where ketoconazole forms a complex with the enzyme (Figures 23 and 24), the energy levels are too low to suggest a combinatorial inhibitory effect with ketoconazole. However, when ketoconazole interacts with the ilmofosine-enzyme complex, the binding energy and intermolecular energy remain almost unchanged (Tables 14 and 15), despite the proximity of ilmofosine (Figures 25 and 26). Notably, in the results shown in Table 14, it can even be observed that the binding and intermolecular energies became stronger. This indicates a cooperative binding interaction, where the presence of ilmofosine potentially enhance and stabilize the binding of ketoconazole, allowing it to effectively bind and exert its therapeutic effect even in close proximity to ilmofosine (62,63).

**Table 16. Interaction Analysis of Ilmofosine and Sterol 24-C-methyltransferase from *T. cruzi* with Ketoconazole bound in Phe95**

Conformations	1	2	3	4	5
Binding Energy (kcal/mol)	-4.5	-2	-1.7	-1.3	-1.08
Intermolecular Energy (kcal/mol)	-12.26	-9.76	-9.46	-9.06	-8.84
Hydrogen Bonds	Tyr94	Tyr94	Lys105	Tyr94	
Distance (Å)	1.922	2.036	1.985	1.85	
Hydrogen Bonds		Asp64 : O	Lys105		
Distance (Å)			1.808		

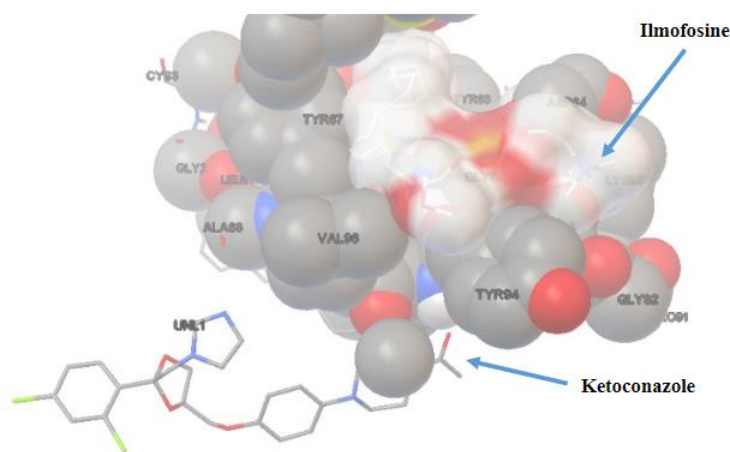


Figure 27: Strongest interaction of Ilmofosine and Sterol 24-C-methyltransferase from *T. cruzi* with Ketoconazole bound in its most likely position. Own authorship.

**Table 17. Interaction Analysis of Ilmofosine and Sterol 24-C-methyltransferase from *T. cruzi* with Ketoconazole bound in Leu97**

Conformations	1	2	3	4	5
Binding Energy (kcal/mol)	-4.71	-3.23	-2.19	-1.11	-1
Intermolecular Energy (kcal/mol)	-12.47	-10.99	-9.95	-8.87	-8.76
Hydrogen Bonds	Tyr67	Lys105		Lys105	
Distance (Å)	2.162	1.612		2.164	
Hydrogen Bonds	Leu1				
Distance (Å)	2.025				
Hydrogen Bonds	Leu1				
Distance (Å)	1.763				

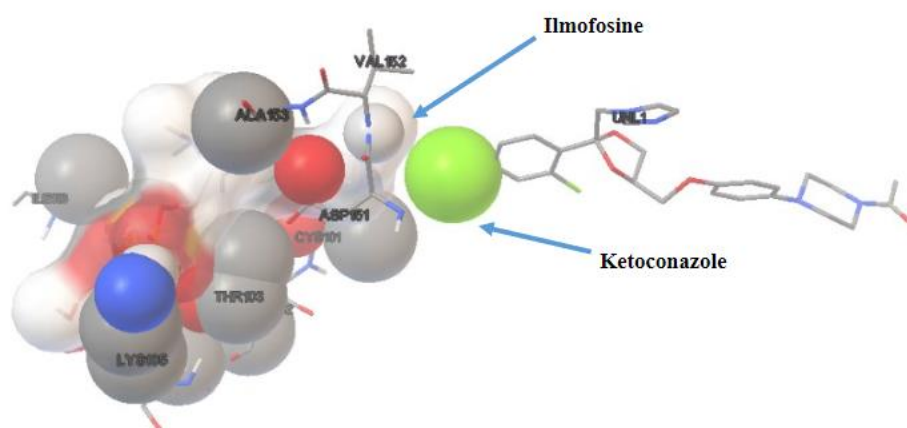


Figure 28: Strongest interaction of Ilmofosine and Sterol 24-C-methyltransferase from *T. cruzi* with Ketoconazole bound to a common Hydrogen Bond site. Own authorship.

**Table 18. Interaction Analysis of Ketoconazole and Sterol 24-C-methyltransferase from *T. cruzi* with Ilmofosine bound in Phe95**

Conformations	1	2	3	4	5
Binding Energy (kcal/mol)	-7.91	-7.9	-7.69	-7.68	-7.52
Intermolecular Energy (kcal/mol)	-10	-9.99	-9.78	-9.76	-9.6
Hydrogen Bonds	Tyr94	Asp151		Gly92	Tyr94
Distance (Å)	1.665	2.62		2.204	1.75

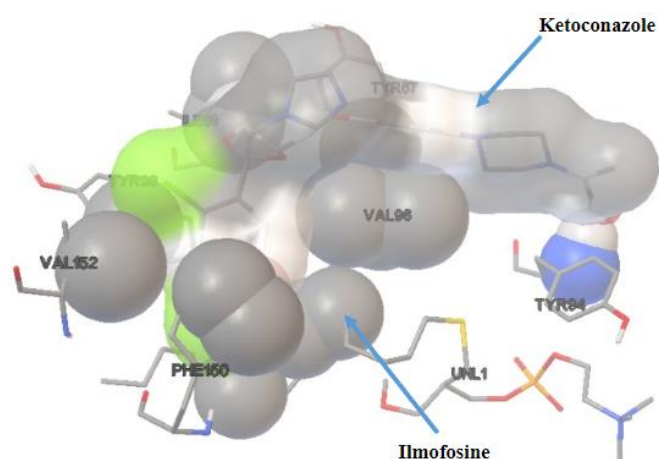


Figure 29: Strongest interaction of Ketoconazole and Sterol 24-C-methyltransferase from *T. cruzi* with Ilmofosine bound in its most likely position. Own authorship.

**Table 19. Interaction Analysis of Ketoconazole and Sterol 24-C-methyltransferase from *T. cruzi* with Ilmofosine bound in Leu97**

Conformations	1	2	3	4	5
Binding Energy (kcal/mol)	-8.84	-8.54	-8.42	-8.4	-8.35
Intermolecular Energy (kcal/mol)	-10.93	-10.63	-10.51	-10.49	-10.44
Hydrogen Bonds	Tyr94		Tyr67	Tyr94	Met21
Distance (Å)	2.958		2.222	2.761	1.963
Hydrogen Bonds					GLY65 : O

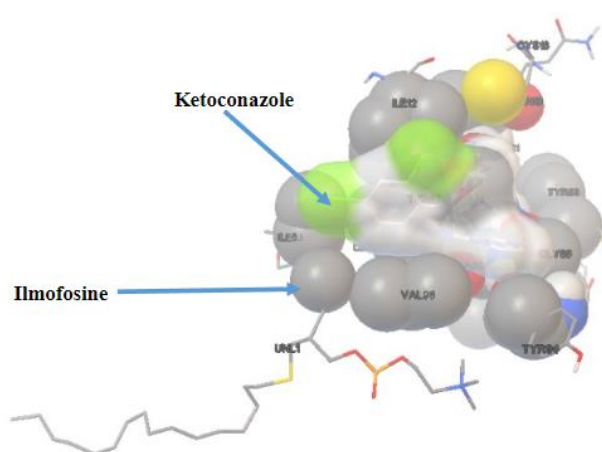


Figure 30: Strongest interaction of Ketoconazole and Sterol 24-C-methyltransferase from *T. cruzi* with Ilmofosine bound to a common Hydrogen Bond site. Own authorship.

As observed from Table 5, the binding of ilmofosine with Sterol 24-C-methyltransferase showed unexpectedly moderate binding energy and strong intermolecular energy. Even in the presence of ketoconazole forming a complex with the enzyme beforehand (Figures 27 and 28),

ilmofosine still exhibits strong intermolecular energy and maintains a similar binding energy with the complex (Tables 16 and 17). This suggests a favorable binding environment and potential synergistic effects with ketoconazole, contributing to the stability and potentially enhancing the inhibitory effect. On the other hand, the presence of ilmofosine lowers the binding and intermolecular energy of ketoconazole's interactions with the enzyme (Figures 29 and 30), although these interactions remain strong (Tables 18 and 19). Therefore, ketoconazole's individual affinity continues to make it a viable candidate for exerting therapeutic effects against Chagas disease.

Initially, the study hypothesized that combining ilmofosine and ketoconazole would produce a synergistic effect due to their distinct mechanisms of action targeting different enzymes. Ilmofosine inhibits PEMT via the Bremer-Greenberg transmethylation pathway, while ketoconazole inhibits both sterol 14 $\alpha$ -demethylase and sterol 24-C-methyltransferase in the ergosterol biosynthesis pathway. However, upon analyzing all the results, it can be speculated that, in addition to each drug acting through its respective pathway, they also influence each other's pathways. These drugs engage in cooperative binding, mutually stabilizing each other and enhancing their combined inhibitory action on the enzyme. This dual interaction suggests that the combination of these drugs exhibits synergistic activity not only within their individual pathways but also across each other's pathways. This highlights their potential as a powerful combined therapeutic agent against Chagas disease.

## 5. Conclusions

The results of our study provide significant insights into the potential therapeutic effects of ilmofosine and ketoconazole, both individually and in combination, against *Trypanosoma cruzi* amastigotes. Through a series of experiments, we established the effective concentrations of each drug and demonstrated a notable synergistic effect when used together. Ilmofosine effectively inhibited *T. cruzi* amastigotes at a concentration of 1  $\mu\text{M}$ , while ketoconazole achieved total eradication of amastigotes at 4 nM. When combined, ilmofosine at 0.2  $\mu\text{M}$  and ketoconazole at 2 nM significantly enhanced their inhibitory effects on amastigote replication.

The combination of these drugs was first evaluated using two-way ANOVA, which revealed statistically significant effects of drug type and concentration, as well as their interaction on the inhibition of *T. cruzi* amastigotes, with p-values substantially lower than the threshold of 0.05. This finding confirms that both factors meaningfully contribute to reducing amastigote replication. Subsequently, the Bliss independence model was applied to predict the expected combined effect based on the independent actions of the drugs. The observed inhibition consistently exceeded these predictions, further supporting the presence of a synergistic interaction. Finally, the Fractional Inhibitory Concentration Index was calculated, yielding a value of 0.7. When plotted on an isobologram according to Loewe's Additivity model, this value fell below the additive curve, confirming that the combination of these drugs is synergistic, achieving greater efficacy at lower concentrations than either drug used alone.

Further insights were gained through molecular docking simulations, which showed strong binding interactions between the drugs and their target enzymes. Ketoconazole demonstrated high binding affinity and intermolecular energy with sterol 14 $\alpha$ -demethylase and sterol 24-C-methyltransferase, both of which are essential enzymes in the ergosterol biosynthesis pathway of *Trypanosoma cruzi*. On the other hand, ilmofosine displayed moderate binding energy but significant intermolecular interactions with phosphatidylethanolamine N-methyltransferase (PEMT) in the phosphatidylcholine biosynthesis pathway, particularly through the Bremer-Greenberg transmethylation pathway. Interestingly, when both drugs were docked to the same protein, they appeared to stabilize each other, particularly when their binding sites were in close proximity. This cooperative interaction could result in a more potent and prolonged inhibitory effect than when the drugs are used individually. This effect was especially pronounced with ketoconazole on sterol 14 $\alpha$ -demethylase in the presence of ilmofosine, and similarly with ilmofosine on PEMT when ketoconazole was present. The observed increase in binding energy in these combinations highlights their potential as synergistic inhibitors against Chagas disease.

In summary, the combination of ilmofosine and ketoconazole offers a promising approach to treating Chagas disease. This synergistic interaction not only boosts the overall effectiveness of the treatment but also has the potential to reduce side effects by lowering the necessary drug dosages. Given the prevalence of Chagas disease in regions like Latin America, this combination therapy could have a significant public health impact. Future research should prioritize in vivo studies, investigate resistance mechanisms, and explore the pharmacokinetics

of these drugs to optimize dosing strategies. Animal model studies will be essential to verify the efficacy and safety of this combination therapy.



## 6. References

1. Macaluso G, Grippi F, Di Bella S, Blanda V, Gucciardi F, Torina A, et al. A Review on the Immunological Response against *Trypanosoma cruzi*. *Pathogens*. 2023 Feb 8;12(2):282.
2. Martín-Escolano J, Marín C, Rosales MJ, Tsaousis AD, Medina-Carmona E, Martín-Escolano R. An Updated View of the *Trypanosoma cruzi* Life Cycle: Intervention Points for an Effective Treatment. *ACS Infect Dis*. 2022 Jun 10;8(6):1107–15.
3. World Health Organization. Chagas disease (also known as American trypanosomiasis). 2024.
4. Lidani KCF, Andrade FA, Bavia L, Damasceno FS, Beltrame MH, Messias-Reason IJ, et al. Chagas Disease: From Discovery to a Worldwide Health Problem. *Front Public Health*. 2019 Jul 2;7.
5. Peña-Callejas G, González J, Jiménez-Cortés JG, De Fuentes-Vicente JA, Salazar-Schettino PM, Bucio-Torres MI, et al. Enfermedad de Chagas: biología y transmisión de *Trypanosoma cruzi*. *TIP Revista Especializada en Ciencias Químico-Biológicas*. 2022 Jun 18;25.
6. Khan AA, Langston HC, Walsh L, Roscoe R, Jayawardhana S, Francisco AF, et al. Enteric nervous system regeneration and functional cure of experimental digestive Chagas disease with trypanocidal chemotherapy. *Nat Commun*. 2024 May 23;15(1):4400.
7. World Health Organization. WHO. 2024. World Chagas Disease Day 2024: urging early diagnosis and care for life.
8. Alves AA, Alcantara CL, Dantas-Jr MVA, Sunter JD, De Souza W, Cunha-e-Silva NL. Dynamics of the orphan myosin MyoF over *Trypanosoma cruzi* life cycle and along the endocytic pathway. *Parasitol Int*. 2022 Feb;86:102444.
9. Barrias E, Zuma A, de Souza W. Life Cycle of Pathogenic Protists: *Trypanosoma cruzi*. In 2022. p. 1–97.
10. Alves AA, Bastin P. The hows and whys of amastigote flagellum motility in *Trypanosoma cruzi*. *mBio*. 2023 Jun 6;
11. National Center for Emerging and Zoonotic Infectious Diseases (NCEZID) D of PD and M. Centers for Disease Control and Prevention . 2021. American Trypanosomiasis.
12. Monje-Rumi MM, Florida-Yapur N, Zago MP, Ragone PG, Pérez Brandán CM, Nuñez S, et al. Potential association of *Trypanosoma cruzi* DTUs TcV and TcVI with

- the digestive form of Chagas disease. *Infection, Genetics and Evolution*. 2020 Oct;84:104329.
13. De Rycker M, Wyllie S, Horn D, Read KD, Gilbert IH. Anti-trypanosomatid drug discovery: progress and challenges. *Nat Rev Microbiol*. 2023 Jan 22;21(1):35–50.
  14. Rassi A, de Rezende JM, Luquetti AO, Rassi A. Clinical phases and forms of Chagas disease. In: *American Trypanosomiasis Chagas Disease*. Elsevier; 2017. p. 653–86.
  15. Liu Z, Ulrich vonBargen R, Kendrick AL, Wheeler K, Leão AC, Sankaranarayanan K, et al. Localized cardiac small molecule trajectories and persistent chemical sequelae in experimental Chagas disease. *Nat Commun*. 2023 Oct 25;14(1):6769.
  16. Pérez-Molina JA, Crespillo-Andújar C, Bosch-Nicolau P, Molina I. Trypanocidal treatment of Chagas disease. *Enferm Infecc Microbiol Clin*. 2021 Nov;39(9):458–70.
  17. García-Huertas P, Cardona-Castro N. Advances in the treatment of Chagas disease: Promising new drugs, plants and targets. *Biomedicine & Pharmacotherapy*. 2021 Oct;142:112020.
  18. Lascano F, García Bournissen F, Altcheh J. Review of pharmacological options for the treatment of Chagas disease. *Br J Clin Pharmacol*. 2022 Feb 6;88(2):383–402.
  19. Soeiro M de NC. Perspectives for a new drug candidate for Chagas disease therapy. *Mem Inst Oswaldo Cruz*. 2022;117.
  20. Martín-Escolano J, Medina-Carmona E, Martín-Escolano R. Chagas Disease: Current View of an Ancient and Global Chemotherapy Challenge. *ACS Infect Dis*. 2020 Nov 13;6(11):2830–43.
  21. Ribeiro V, Dias N, Paiva T, Hagström-Bex L, Nitz N, Pratesi R, et al. Current trends in the pharmacological management of Chagas disease. *Int J Parasitol Drugs Drug Resist*. 2020 Apr;12:7–17.
  22. Santa-Rita RM, Henriques-Pons A, Barbosa HS, de Castro SL. Effect of the lysophospholipid analogues edelfosine, ilmofosine and miltefosine against *Leishmania amazonensis*. *Journal of Antimicrobial Chemotherapy*. 2004 Oct 1;54(4):704–10.
  23. APT B W, ZULANTAY A I. Estado actual en el tratamiento de la enfermedad de Chagas. *Rev Med Chil*. 2011 Feb;139(2):247–57.
  24. Azzouz S, Maache M, Garcia RG, Osuna A. Leishmanicidal Activity of Edelfosine, Miltefosine and Ilmofosine. *Basic Clin Pharmacol Toxicol*. 2005 Jan 24;96(1):60–5.
  25. Shirley M. Ketoconazole in Cushing’s syndrome: a profile of its use. *Drugs & Therapy Perspectives*. 2021 Feb 7;37(2):55–64.

26. Mazzeti AL, Capelari-Oliveira P, Bahia MT, Mosqueira VCF. Review on Experimental Treatment Strategies Against *Trypanosoma cruzi*. *J Exp Pharmacol*. 2021 Mar;Volume 13:409–32.
27. Santos SS, de Araújo RV, Giarolla J, Seoud O El, Ferreira EI. Searching for drugs for Chagas disease, leishmaniasis and schistosomiasis: a review. *Int J Antimicrob Agents*. 2020 Apr;55(4):105906.
28. Osorio-Méndez JF, Cevallos AM. Discovery and Genetic Validation of Chemotherapeutic Targets for Chagas' Disease. *Front Cell Infect Microbiol*. 2019 Jan 7;8.
29. Makurvet FD. Biologics vs. small molecules: Drug costs and patient access. *Med Drug Discov*. 2021 Mar;9:100075.
30. Beltran-Hortelano I, Alcolea V, Font M, Pérez-Silanes S. Examination of multiple *Trypanosoma cruzi* targets in a new drug discovery approach for Chagas disease. *Bioorg Med Chem*. 2022 Mar;58:116577.
31. Booth LA, Smith TK. Lipid metabolism in *Trypanosoma cruzi*: A review. *Mol Biochem Parasitol*. 2020 Nov;240:111324.
32. Li J, Xin Y, Li J, Chen H, Li H. Phosphatidylethanolamine N-methyltransferase: from Functions to Diseases. *Aging Dis*. 2023;14(3):879.
33. Saito R de F, Andrade LN de S, Bustos SO, Chammas R. Phosphatidylcholine-Derived Lipid Mediators: The Crosstalk Between Cancer Cells and Immune Cells. *Front Immunol*. 2022 Feb 15;13.
34. Ramaprasad A, Burda PC, Calvani E, Sait AJ, Palma-Duran SA, Withers-Martinez C, et al. A choline-releasing glycerophosphodiesterase essential for phosphatidylcholine biosynthesis and blood stage development in the malaria parasite. *Elife*. 2022 Dec 28;11.
35. Piñeiro M, Ortiz JE, Spina Zapata RM, Barrera PA, Sosa MA, Roitman G, et al. Antiparasitic Activity of *Hippeastrum* Species and Synergistic Interaction between Montanine and Benznidazole against *Trypanosoma cruzi*. *Microorganisms*. 2023 Jan 6;11(1):144.
36. Gulin JEN, Eagleson MA, López-Muñoz RA, Solana ME, Altcheh J, García-Bournissen F. In vitro and in vivo activity of voriconazole and benznidazole combination on *trypanosoma cruzi* infection models. *Acta Trop*. 2020 Nov;211:105606.
37. Schloer S, Brunotte L, Mecate-Zambrano A, Zheng S, Tang J, Ludwig S, et al. Drug synergy of combinatory treatment with remdesivir and the repurposed drugs fluoxetine

- and itraconazole effectively impairs SARS-CoV-2 infection in vitro. *Br J Pharmacol*. 2021 Jun 6;178(11):2339–50.
38. Zou H, Ye H, Kamaraj R, Zhang T, Zhang J, Pavek P. A review on pharmacological activities and synergistic effect of quercetin with small molecule agents. *Phytomedicine*. 2021 Nov;92:153736.
  39. Bobrowski T, Chen L, Eastman RT, Itkin Z, Shinn P, Chen CZ, et al. Synergistic and Antagonistic Drug Combinations against SARS-CoV-2. *Molecular Therapy*. 2021 Feb;29(2):873–85.
  40. Duarte D, Vale N. Evaluation of synergism in drug combinations and reference models for future orientations in oncology. *Current Research in Pharmacology and Drug Discovery*. 2022;3:100110.
  41. Assaad HI, Hou Y, Zhou L, Carroll RJ, Wu G. Rapid publication-ready MS-Word tables for two-way ANOVA. *Springerplus*. 2015 Dec 23;4(1):33.
  42. Slinker BK. The Statistics of Synergism. *J Mol Cell Cardiol*. 1998 Apr;30(4):723–31.
  43. Zhao W, Sachsenmeier K, Zhang L, Sult E, Hollingsworth RE, Yang H. A New Bliss Independence Model to Analyze Drug Combination Data. *SLAS Discovery*. 2014 Jun;19(5):817–21.
  44. Onyekachukwu Izuchukwu Udemezue, Christian Chibuzo Uba, Onyekachi Ijeoma Udemezue, Evangeline Chinyere Udenweze, Joachim Ohiakwu Ezeadila, Chijioke Obinna Ezenwelu. Combined activity of blue vitriol, brimstone and black stone on clinical *Candida* species isolates using fractional inhibitory concentration Index. *International Journal of Biological and Pharmaceutical Sciences Archive*. 2024 May 30;7(2):050–6.
  45. Fatsis-Kavalopoulos N, Sánchez-Hevia DL, Andersson DI. Beyond the FIC index: the extended information from fractional inhibitory concentrations (FICs). *Journal of Antimicrobial Chemotherapy*. 2024 Jul 13;
  46. Meletiadis J, Pournaras S, Roilides E, Walsh TJ. Defining Fractional Inhibitory Concentration Index Cutoffs for Additive Interactions Based on Self-Drug Additive Combinations, Monte Carlo Simulation Analysis, and *In Vitro* - *In Vivo* Correlation Data for Antifungal Drug Combinations against *Aspergillus fumigatus*. *Antimicrob Agents Chemother*. 2010 Feb;54(2):602–9.
  47. Huang R yue, Pei L, Liu Q, Chen S, Dou H, Shu G, et al. Isobologram Analysis: A Comprehensive Review of Methodology and Current Research. *Front Pharmacol*. 2019 Oct 29;10.

48. Yasuo N, Ishida T, Sekijima M. Computer aided drug discovery review for infectious diseases with case study of anti-Chagas project. *Parasitol Int.* 2021 Aug;83:102366.
49. Beltran-Hortelano I, Alcolea V, Font M, Pérez-Silanes S. Examination of multiple *Trypanosoma cruzi* targets in a new drug discovery approach for Chagas disease. *Bioorg Med Chem.* 2022 Mar;58:116577.
50. Gabaldón-Figueira JC, Martínez-Peinado N, Escabia E, Ros-Lucas A, Chatelain E, Scandale I, et al. State-of-the-Art in the Drug Discovery Pathway for Chagas Disease: A Framework for Drug Development and Target Validation. *Res Rep Trop Med.* 2023 Jun;Volume 14:1–19.
51. Coro-Bermello J, López-Rodríguez ER, Alfonso-Ramos JE, Alonso D, Ojeda-Carralero GM, Prado GA, et al. Identification of novel thiadiazin derivatives as potentially selective inhibitors towards trypanothione reductase from *Trypanosoma cruzi* by molecular docking using the numerical index poses ratio Pr and the binding mode analysis. *SN Appl Sci.* 2021 Mar 25;3(3):376.
52. Yepes AF, Quintero-Saumeth J, Cardona-Galeano W. Biologically Active Quinoline-Hydrazone Conjugates as Potential *Trypanosoma cruzi* DHFR-TS Inhibitors: Docking, Molecular Dynamics, MM/PBSA and Drug-Likeness Studies. *ChemistrySelect.* 2021 Mar 26;6(12):2928–38.
53. Sakyi PO, Broni E, Amewu RK, Miller WA, Wilson MD, Kwofie SK. Homology Modeling, de Novo Design of Ligands, and Molecular Docking Identify Potential Inhibitors of *Leishmania donovani* 24-Sterol Methyltransferase. *Front Cell Infect Microbiol.* 2022 Jun 2;12.
54. Majeux N, Scarsi M, Apostolakis J, Ehrhardt C, Caflisch A. Exhaustive docking of molecular fragments with electrostatic solvation. *Proteins: Structure, Function, and Genetics.* 1999 Oct 1;37(1):88–105.
55. Morris GM, Goodsell DS, Pique ME, Lindstrom W, Huey R, Forli S, et al. Automated Docking of Flexible Ligands to Flexible Receptors [Internet]. 2014. Available from: <http://autodock.scripps.edu/>
56. Chen T, Shu X, Zhou H, Beckford FA, Misir M. Algorithm selection for protein–ligand docking: strategies and analysis on ACE. *Sci Rep.* 2023 May 22;13(1):8219.
57. Rehman MdT, AlAjmi MF, Hussain A. Natural Compounds as Inhibitors of SARS-CoV-2 Main Protease (3CLpro): A Molecular Docking and Simulation Approach to Combat COVID-19. *Curr Pharm Des.* 2021 Oct 12;27(33):3577–89.
58. Qasim R, Thiab TA, Alhindi T, Al-Hunaiti A, Imraish A. The Nurr1 ligand indole acetic acid hydrazide loaded onto ZnFe<sub>2</sub>O<sub>4</sub> nanoparticles suppresses proinflammatory gene expressions in SimA9 microglial cells. *Sci Rep.* 2024 Jun 17;14(1):13987.

59. Kodidela S, Shaik FB, Mittameedi CM, Chintha V, Nallanchakravarthula V. Alcohol exacerbated biochemical and biophysical alterations in liver mitochondrial membrane of diabetic male wistar rats – A possible amelioration by green tea. *Clinical Nutrition Open Science*. 2022 Apr;42:130–47.
60. Rojas Vargas JA, López AG, Pérez Y, Cos P, Froeyen M. In vitro evaluation of arylsubstituted imidazoles derivatives as antiprotozoal agents and docking studies on sterol 14 $\alpha$ -demethylase (CYP51) from *Trypanosoma cruzi*, *Leishmania infantum*, and *Trypanosoma brucei*. *Parasitol Res*. 2019 May 23;118(5):1533–48.
61. Nes WD. Biosynthesis of Cholesterol and Other Sterols. *Chem Rev*. 2011 Oct 12;111(10):6423–51.
62. Sykes DA, Stoddart LA, Kilpatrick LE, Hill SJ. Binding kinetics of ligands acting at GPCRs. *Mol Cell Endocrinol*. 2019 Apr;485:9–19.
63. Stefan MI, Le Novère N. Cooperative Binding. *PLoS Comput Biol*. 2013 Jun 27;9(6):e1003106.